

Rheology of a dilute emulsion of surfactant-covered spherical drops

J. Bławdziewicz¹, P. Vlahovska, M. Loewenberg

*Department of Chemical Engineering, Yale University, P.O. Box 208286,
New Haven, CT 06520-8286, USA*

Received 29 June 1999; received in revised form 14 July 1999

Abstract

The rheology of a diluted emulsion of surfactant-covered spherical drops has been investigated. A diluted film of insoluble surfactant is assumed. A matrix formulation of the problem is derived and analyzed by perturbation expansions for low- and high-shear rates, and for high-viscosity drops; the high-viscosity expansion converges rapidly for a wide range of parameters. Our theory provides a quantitative description of shear thinning and normal stress differences that occur as a result of surfactant redistribution. © 2000 Elsevier Science B.V. All rights reserved.

PACS: 82.70.Kj; 83.50.Gd; 47.15.Gf; 83.50.Lh

Keywords: Emulsion; Surfactant; Rheology; Stokes flow

1. Introduction

Emulsion rheology has been the subject of many investigations which are reviewed in Refs. [1,2]. Linear and nonlinear viscoelastic properties have been studied [3–5], and numerical simulations of emulsions of deformable drops are being developed [6,7].

An understanding of the effects of surfactant on drop dynamics and emulsion rheology is at an earlier stage, although this has been the focus of some recent studies. Palierne [8] included surfactants in a theoretical description of the linear viscoelastic spectrum of dilute emulsions. The dynamics of spherical drops covered with an incompressible surfactant film was explored by Bławdziewicz et al. [9]. Pozrikidis and coworkers [10,11] developed numerical simulations for the dynamics of deformable

¹ Fax: +1-203-432-4594.

E-mail address: jerzy@stokes.eng.yale.edu (J. Bławdziewicz)

surfactant-covered drops. However, despite the recent progress, a fundamental understanding of the nonlinear effects of surfactants on emulsion rheology is unavailable.

The complicating effects of surfactants stem from the dependence of surface tension on the interfacial concentration of surfactant. The evolution of the surfactant distribution is nonlinearly coupled to the flow field through the tangential stress discontinuity at the interface, resulting from flow-induced surface tension gradients (Marangoni stresses). Adsorbed surfactant also influences the normal stress balance by reducing surface tension.

When the capillary pressure dominates viscous stresses generated by the flow, drops remain nearly spherical. Under these conditions, adsorbed surfactant influences drop dynamics only through tangential Marangoni stresses. When drop deformation is slight, the surfactant concentration often remains nearly uniform, i.e., the surfactant film is incompressible [9,12]. In this case, an isolated drop in a linear flow behaves as a rigid particle thus, a Newtonian rheology is predicted for a dilute emulsion.

However, significant surfactant redistribution is possible even for undeformed drops if the elasticity of the surfactant film is low [13] (e.g., low interfacial surfactant concentrations). Thus, drop dynamics depend on the external flow field as well as the instantaneous distribution of surfactant, and the rheology of the emulsion is non-Newtonian. This paper describes an investigation of the dynamics of surfactant-covered spherical drops under conditions where surfactant redistribution is appreciable.

The problem is presented in Section 2, including our assumptions, a dimensional analysis, and the formulation of the relevant boundary value problem. The problem is recast in integral form in Section 3, and the surfactant contribution to the average stress in a dilute emulsion is expressed as an integral of the surfactant distribution. In Section 4, the equations are rewritten in a matrix representation using the formalism developed by Felderhof and coworkers [14]. A quadratic matrix equation is obtained that describes the evolution of the surfactant distribution. The quadratic term results from the nonlinear coupling in the surfactant conservation equation between the fluid velocity and the surfactant concentration.

Analytical results for the rheology of a dilute emulsion of surfactant-covered drops are derived in Section 5 by a perturbation analysis for low- and high-shear rates, and for high-viscosity drops. In Section 6, numerical solution of the matrix equation is described. The results are discussed in Section 7, and concluding remarks are made in Section 8.

2. Dilute emulsion of surfactant-covered drops

2.1. Assumptions

We consider a dilute emulsion of spherical drops with radius a and viscosity $\lambda\eta$, embedded in an ambient fluid with viscosity η . Creeping-flow conditions are assumed.

A diluted surfactant film is adsorbed on the drop interfaces; the surfactant is insoluble in the bulk phases and is non-diffusing. The average surfactant concentration on the drop interface is Γ_{eq} . The corresponding interfacial tension is σ_{eq} , and σ_0 is the interfacial tension in the absence of surfactant.

The emulsion undergoes a linear flow with strain-rate magnitude $\dot{\gamma}$. The characteristic stress associated with the flow is $\tau_\eta = \eta\dot{\gamma}$. The magnitude of drop deformation depends on the capillary number

$$Ca = \frac{\tau_\eta a}{\sigma_{\text{eq}}}, \quad (1)$$

which is the ratio of viscous to capillary stresses. The magnitude of surfactant redistribution is determined by the inverse Marangoni number

$$Ma^{-1} = \frac{\tau_\eta a}{\Delta\sigma}, \quad (2)$$

which is the ratio of viscous stresses to the characteristic Marangoni stresses, where $\Delta\sigma = \sigma_0 - \sigma_{\text{eq}}$.

The focus of this paper is on systems where surfactant redistribution on drop interfaces is significant, but drop deformation is negligible. Therefore, we assume

$$Ca \ll 1 \quad (3)$$

and

$$Ma = O(1). \quad (4)$$

Conditions (3) and (4) imply low elasticity of the surfactant film,

$$\frac{\Delta\sigma}{\sigma_{\text{eq}}} \ll 1, \quad (5)$$

which occurs for low surfactant concentrations. Therefore, a linear “perfect gas” interfacial equation of state is here assumed, and surface viscosity is neglected. The results presented in this paper indicate that small amounts of adsorbed surfactant can significantly affect emulsion rheology.

Herein, the surfactant concentration is normalized by Γ_{eq} ; all other quantities are rescaled using η , a , and $\dot{\gamma}$. Accordingly, the time scale is $\dot{\gamma}^{-1}$, the velocity scale is $\dot{\gamma}a$, bulk stresses are scaled with τ_η , and the scale for interfacial tension is $\tau_\eta a$.

2.2. Rheology

We consider a dilute emulsion in an external linear flow

$$\mathbf{u}_\infty = \mathbf{E} \cdot \mathbf{r}, \quad (6)$$

where the traceless velocity-gradient tensor \mathbf{E} is independent of position \mathbf{r} , but may be time dependent. The symmetric part \mathbf{E}^s of the gradient tensor describes the straining component of the flow,

$$\mathbf{u}_\infty^s = \mathbf{E}^s \cdot \mathbf{r}, \quad (7)$$

and the antisymmetric part \mathbf{E}^A describes the rigid-body rotation

$$\mathbf{u}_\infty^r = \boldsymbol{\Omega} \times \mathbf{r} \tag{8}$$

with the angular velocity components

$$\Omega_i = -\frac{1}{2} \varepsilon_{ijk} E_{jk}^A, \tag{9}$$

where ε_{ijk} is the alternating unit tensor.

Effective rheological properties of a dilute emulsion can be derived from a solution \mathbf{u} of a Stokes-flow problem for an isolated drop in the external flow \mathbf{u}_∞ . For an emulsion with drop volume fraction ϕ in a linear flow (6), the traceless part of the average stress tensor is

$$\boldsymbol{\Sigma} = 2\mathbf{E}^s + \phi\boldsymbol{\tau}^d, \tag{10}$$

where

$$\boldsymbol{\tau}^d = -\frac{3}{4\pi} \mathcal{F} \tag{11}$$

is the drop contribution to the stress, and

$$\mathcal{F}_{ij} = \frac{1}{2} \int [r_i f_j(\mathbf{r}) + r_j f_i(\mathbf{r}) - \frac{2}{3} \delta_{ij} \mathbf{r} \cdot \mathbf{f}(\mathbf{r})] d\mathbf{r} \tag{12}$$

is the traceless symmetric dipole moment of the induced force distribution (stresslet) [15–18]. By definition, the induced force distribution $\mathbf{f}(\mathbf{r})$ acting in a uniform fluid generates the same disturbance flow $\mathbf{u} - \mathbf{u}_\infty$ as produced by the drop. For surfactant-covered drops, $\mathbf{f}(\mathbf{r})$ depends on the external flow and the instantaneous distribution of surfactant.

For a stationary shear flow in the x - y plane, with the velocity in the x direction, the components of the tensor \mathbf{E} in Eq. (6) are

$$E_{ij} = \delta_{i1} \delta_{j2}. \tag{13}$$

In this flow, the drop contribution to the effective stress tensor is fully characterized by the shear stress and two normal stress differences. By the linearity of the Stokes equations, the drop contribution to the shear stress consists of two parts,

$$\tau_{12}^d = \tau_{12}^0 + \tau_{12}^r, \tag{14}$$

where

$$\tau_{12}^0 = \frac{5}{2} - \frac{3}{2} \lambda_1^{-1} \tag{15}$$

is the contribution corresponding to a drop with a surfactant-free interface [19], and

$$\lambda_1 = \lambda + 1. \tag{16}$$

The extra contribution resulting from the presence of surfactant is τ_{12}^r . The first and second normal stress differences

$$N_1 = \tau_{11}^d - \tau_{22}^d, \quad N_2 = \tau_{22}^d - \tau_{33}^d. \tag{17}$$

result solely from the presence of surfactant.

In the next section we formulate evolution equations describing the motion of a surfactant-covered spherical drop in an external flow.

2.3. Boundary-value problem

The motion of a surfactant-covered spherical drop depends on two coupled processes: (1) the evolution of the surfactant distribution Γ for a given interfacial velocity, and (2) the flow field \mathbf{u} generated by the external flow and a given (instantaneous) distribution of surfactant. We formulate the corresponding subproblems in a reference frame with the drop center at $\mathbf{r} = 0$, and the drop interface at $r = 1$, where $r = |\mathbf{r}|$.

The evolution of an insoluble, non-diffusing surfactant is governed by the interfacial continuity equation

$$\frac{\partial \Gamma}{\partial t} + \nabla_s \cdot (\Gamma \mathbf{u}_s) = 0, \quad (18)$$

where ∇_s denotes the surface gradient operator, and \mathbf{u}_s is the interfacial velocity.

Fluid motion on both sides of the interface is described by the Stokes equations,

$$\bar{\eta}_i \nabla^2 \mathbf{u} - \nabla p = 0, \quad \nabla \cdot \mathbf{u} = 0, \quad (19)$$

where $i = 1, 2$, and the dimensionless viscosity of the outside fluid is $\bar{\eta}_1 = 1$ and the inside fluid is $\bar{\eta}_2 = \lambda$. Fluid velocity is continuous across the interface,

$$\mathbf{u}_{\text{out}} = \mathbf{u}_{\text{in}} = \mathbf{u}_s, \quad (20)$$

where the subscript out (in) denotes positions just outside (inside) the interface. The boundary condition for the normal velocity component is

$$\hat{\mathbf{r}} \cdot \mathbf{u}_s = 0, \quad (21)$$

where $\hat{\mathbf{r}} = \mathbf{r}/r$. At infinity the flow tends to the incident flow,

$$\mathbf{u} \rightarrow \mathbf{u}_\infty. \quad (22)$$

The discontinuity of the tangential traction across the interface is balanced by the gradient of surface tension $\sigma(\Gamma)$,

$$\mathbf{I}_s \cdot (\mathbf{t}_{\text{out}} - \mathbf{t}_{\text{in}}) = -\nabla_s \sigma, \quad (23)$$

where $\mathbf{t} = \boldsymbol{\tau} \cdot \hat{\mathbf{r}}$ is the traction, $\boldsymbol{\tau}$ is the stress tensor, and $\mathbf{I}_s = \mathbf{I} - \hat{\mathbf{r}}\hat{\mathbf{r}}$ is the surface projection operator. Surface tension is related to the surfactant concentration through the perfect-gas equation of state. In dimensionless variables, the relation is

$$\sigma(\Gamma) = \sigma(1) - Ma\bar{F}, \quad (24)$$

where the Marangoni number is defined by Eq. (2) with $\Delta\sigma = k_B T \Gamma_{\text{eq}}$ (k_B is Boltzmann's constant, T is temperature) and \bar{F} is the deviation of the surfactant concentration from the equilibrium value,

$$\Gamma = 1 + \bar{F}. \quad (25)$$

3. Integral formulation

3.1. Induced force

Boundary conditions (22), (23) and equation of state (24) imply that the induced force distribution \mathbf{f} is linear in \mathbf{u}_∞ and $\bar{\Gamma}$,

$$\mathbf{f} = -\widehat{\mathbf{Z}}\mathbf{u}_\infty + Ma\widehat{\mathbf{M}}\bar{\Gamma}, \tag{26}$$

where

$$[\widehat{\mathbf{Z}}\mathbf{u}_\infty](\mathbf{r}) = \int \mathbf{Z}(\mathbf{r}, \mathbf{r}') \cdot \mathbf{u}_\infty(\mathbf{r}') \, d\mathbf{r}' \tag{27}$$

and

$$[\widehat{\mathbf{M}}\bar{\Gamma}](\mathbf{r}) = \int \mathbf{M}(\mathbf{r}, \mathbf{r}')\bar{\Gamma}(\mathbf{r}') \, d\mathbf{r}'. \tag{28}$$

Without loss of generality for the problem considered herein, we assume that the induced force distribution and the integral kernels $\mathbf{A} = \mathbf{Z}, \mathbf{M}$ are confined to the drop surface,

$$\mathbf{f}(\mathbf{r}) = \delta(r - 1)\mathbf{f}_s(\hat{\mathbf{r}}), \tag{29}$$

and

$$\mathbf{A}(\mathbf{r}, \mathbf{r}') = \mathbf{A}_s(\hat{\mathbf{r}}, \hat{\mathbf{r}}')\delta(r - 1)\delta(r' - 1). \tag{30}$$

By the Lorentz reciprocal theorem

$$Z_{\alpha\beta}(\mathbf{r}, \mathbf{r}') = Z_{\beta\alpha}(\mathbf{r}', \mathbf{r}). \tag{31}$$

Matrix representations of the integral operators $\widehat{\mathbf{Z}}$ and $\widehat{\mathbf{M}}$ are given in Section 4.

3.2. Fluid velocity and surfactant transport

The fluid velocity inside and outside the drop is the solution of Stokes equations in a uniform fluid with the induced force distribution \mathbf{f} . Accordingly,

$$\mathbf{u} = \mathbf{u}_\infty + \widehat{\mathbf{T}}_0\mathbf{f}, \tag{32}$$

where

$$[\widehat{\mathbf{T}}_0\mathbf{f}](\mathbf{r}) = \int \mathbf{T}_0(\mathbf{r} - \mathbf{r}') \cdot \mathbf{f}(\mathbf{r}') \, d\mathbf{r}', \tag{33}$$

and

$$\mathbf{T}_0(\mathbf{r}) = \frac{1}{8\pi r}(\mathbf{I} + \hat{\mathbf{r}}\hat{\mathbf{r}}) \tag{34}$$

is the Oseen tensor.

By inserting (26) and (32) into the conservation equation (18), the evolution equation for the surfactant distribution

$$\frac{\partial \bar{\Gamma}}{\partial t} = -\nabla_s \cdot \Gamma(1 + \widehat{\mathbf{X}})\mathbf{u}_\infty - Ma\nabla_s \cdot \Gamma\widehat{\mathbf{W}}\bar{\Gamma} \tag{35}$$

is obtained, where

$$\widehat{\mathbf{X}} = -\widehat{\mathbf{T}}_0 \widehat{\mathbf{Z}}, \quad (36)$$

$$\widehat{\mathbf{W}} = \widehat{\mathbf{T}}_0 \widehat{\mathbf{M}}. \quad (37)$$

The quantities on the right-hand side of (35) are evaluated at $r = 1$. A matrix representation of Eq. (35) is derived below.

4. Matrix representations

Explicit representations of the hydrodynamic operators and the surfactant evolution equation (35) are obtained by expanding scalar and vector fields into the appropriate sets of basis functions.

The surfactant concentration \bar{F} is expanded in scalar spherical harmonics

$$\bar{F} = \sum_{lm} \gamma_{lm} Y_{lm}, \quad (38)$$

where the summation is over the range $l \geq 1$ and $-l \leq m \leq l$. The harmonics Y_{lm} are normalized

$$\langle Y_{lm} \delta_r | Y_{l'm'} \rangle = \delta_{ll'} \delta_{mm'}, \quad (39)$$

where

$$\langle f | g \rangle = \int f^*(\mathbf{r}') g(\mathbf{r}') d\mathbf{r}' \quad (40)$$

(with the asterisk denoting the complex conjugate), and

$$\delta_r = \frac{1}{r^2} \delta(r - r'). \quad (41)$$

In this notation, the expansion coefficients γ_{lm} are given by

$$\gamma_{lm} = \langle Y_{lm} \delta_1 | \bar{F} \rangle. \quad (42)$$

We use two different sets of functions to expand the flow field components and induced force distribution: an adjointed orthonormal basis introduced by Cichocki et al. [14], and a surface representation in terms of velocity fields that are normal and tangential to the drop interface. These are described in the following two subsections.

4.1. Representation in adjointed basis

In this representation, vector fields are expanded using the fundamental sets of solutions of Stokes equations \mathbf{v}_{lmq}^\pm [14], listed in Appendix A, and the adjointed functions \mathbf{w}_{lmq}^\pm that satisfy the orthonormality conditions

$$\langle \mathbf{w}_{lmq}^\pm \delta_r | \mathbf{v}_{l'm'q'}^\pm \rangle = \delta_{ll'} \delta_{mm'} \delta_{qq'} \quad (43)$$

for $r > 0$, where the scalar product of two vector fields is

$$\langle \mathbf{f} | \mathbf{g} \rangle = \int \mathbf{f}^*(\mathbf{r}') \cdot \mathbf{g}(\mathbf{r}') \, d\mathbf{r}' \tag{44}$$

Note that the normalization used herein differs from that used in Ref. [14] (cf. Eqs. (A.18) and (A.19)).

The solutions \mathbf{v}_{lmq}^+ are nonsingular at the origin, and the \mathbf{v}_{lmq}^- are nonsingular at infinity; thus, the expansions of the incident and scattered flows are

$$\mathbf{u}_\infty = \sum_{lmq} c_{lmq}^+ \mathbf{v}_{lmq}^+ \tag{45}$$

and

$$\mathbf{u} - \mathbf{u}_\infty = \sum_{lmq} c_{lmq}^- \mathbf{v}_{lmq}^-, \tag{46}$$

where the summation is over the range $l \geq 1$, $-l \leq m \leq l$, and $0 \leq q \leq 2$. According to (43), the expansion coefficients in the above equations are

$$c_{lmq}^\pm = \langle \mathbf{w}_{lmq}^\pm \delta_1 | \mathbf{u}^\pm \rangle, \tag{47}$$

where $\mathbf{u}^+ = \mathbf{u}_\infty$, and $\mathbf{u}^- = \mathbf{u} - \mathbf{u}_\infty$.

4.1.1. Hydrodynamic operators

In the adjointed basis $\mathbf{v}_{lmq}^\pm, \mathbf{w}_{lmq}^\pm$, solutions for Stokes flow in the presence of a spherically symmetric particle have simple representations that are described below. In this basis, Eq. (26) transforms to equation for the reduced multipole moments of the induced force [14]

$$f_{lmq} = \langle \mathbf{v}_{lmq}^+ | \mathbf{f} \rangle, \tag{48}$$

where

$$f_{lmq} = f_{lmq}^0 + f_{lmq}^F, \tag{49}$$

with flow contribution

$$f_{lmq}^0 = -\langle \mathbf{v}_{lmq}^+ | \widehat{\mathbf{Z}} | \mathbf{v}_{l'm'q'}^+ \rangle c_{l'm'q'}^+, \tag{50}$$

and surfactant contribution

$$f_{lmq}^F = Ma \langle \mathbf{v}_{lmq}^+ | \widehat{\mathbf{M}} | Y_{l'm'} \rangle \gamma_{l'm'}. \tag{51}$$

Summation over the repeated subscripts in Eq. (50) and (51) is implied; we use this convention hereafter.

Since the operators $\widehat{\mathbf{Z}}$ and $\widehat{\mathbf{M}}$ are isotropic, the corresponding matrices are diagonal in angular and azimuthal quantum numbers,

$$\langle \mathbf{v}_{lmq}^+ | \widehat{\mathbf{Z}} | \mathbf{v}_{l'm'q'}^+ \rangle = -\delta_{ll'} \delta_{mm'} X_{qq'}(l), \tag{52}$$

$$\langle \mathbf{v}_{lmq}^+ | \widehat{\mathbf{M}} | Y_{l'm'} \rangle = \delta_{ll'} \delta_{mm'} W_q(l), \tag{53}$$

where, by rotational symmetry, the matrices $X_{qq'}(l)$ and $W_q(l)$ are independent of m . The explicit expression (C.1) for the matrix $X_{qq'}(l)$ has been derived in Ref. [18], and a derivation of expression (C.15) for the matrix $W_q(l)$ is given in Appendix C.

The matrix elements of the operator $\widehat{\mathbf{T}}_0$ are [14]

$$\langle \mathbf{w}_{lmq}^- \delta_1 | \widehat{\mathbf{T}}_0 | \delta_1 \mathbf{w}_{l'm'q'}^+ \rangle = \delta_{ll'} \delta_{mm'} \delta_{qq'}. \quad (54)$$

By combining the above equation with (36) and (52) we find

$$\langle \mathbf{w}_{lmq}^- \delta_1 | \widehat{\mathbf{X}} | \mathbf{v}_{l'm'q'}^+ \rangle = \delta_{ll'} \delta_{mm'} X_{qq'}(l), \quad (55)$$

and with (37) and (53) we find

$$\langle \mathbf{w}_{lmq}^- \delta_1 | \widehat{\mathbf{W}} | Y_{lm} \rangle = \delta_{ll'} \delta_{mm'} W_q(l). \quad (56)$$

4.1.2. Stresslet

To find the relation between stresslet (12) and the induced force multipoles f_{lmq} , we expand \mathcal{F} in the spherical basis \mathbf{a}_{2m} of symmetric second-order traceless tensors,

$$\mathcal{F} = \sum_{m=-2}^2 \mathcal{F}_m \mathbf{a}_{2m}. \quad (57)$$

The basis \mathbf{a}_{2m} is related to the harmonics \mathbf{Y}_{21m} by the formula

$$\mathbf{Y}_{21m} = \left(\frac{4\pi}{3} \right)^{-1/2} \mathbf{a}_{2m} \cdot \hat{\mathbf{r}}, \quad (58)$$

and is orthonormal; explicit formulae are given in Appendix B. By projecting Eq. (12) onto \mathbf{a}_{2m} , and using definitions (48), (58), and (A.10), (A.12) we find

$$\mathcal{F}_m = \left(\frac{2\pi}{15} \right)^{1/2} f_{2m0}. \quad (59)$$

4.1.3. Shear flow

In linear flows (6), the rigid-rotation and the straining components of the external flow, \mathbf{u}_∞^r and \mathbf{u}_∞^s , are characterized by

$$\langle \mathbf{w}_{lmq}^+ \delta_1 | \mathbf{u}_\infty^r \rangle = c_{1m1}^+ \delta_{l1} \delta_{q1}, \quad (60)$$

and

$$\langle \mathbf{w}_{lmq}^+ \delta_1 | \mathbf{u}_\infty^s \rangle = c_{2m0}^+ \delta_{l2} \delta_{q0}. \quad (61)$$

For shear flow (13), the nonzero coefficients of expansion (45) are

$$c_{2\pm 20}^+ = \mp i \sqrt{\frac{\pi}{30}}, \quad c_{101}^+ = i \sqrt{\frac{\pi}{3}}. \quad (62)$$

In terms of the induced force multipoles (48), the expressions for the two contributions to the shear stress (14) are

$$\tau_{12}^0 = -\frac{i}{8}\sqrt{\frac{6}{5\pi}}(f_{220}^0 - f_{2-20}^0), \tag{63}$$

$$\tau_{12}^r = -\frac{i}{8}\sqrt{\frac{6}{5\pi}}(f_{220}^r - f_{2-20}^r). \tag{64}$$

Taylor expression (15) is recovered from Eqs. (50), (52), (62), and (C.1). The normal stress differences (17) are

$$N_1 = -\frac{1}{4}\sqrt{\frac{6}{5\pi}}(f_{220}^r + f_{2-20}^r), \tag{65}$$

$$N_2 = \frac{1}{8}\sqrt{\frac{6}{5\pi}}(f_{220}^r + f_{2-20}^r + \sqrt{6}f_{200}^r). \tag{66}$$

4.2. Representation in surface basis

Normal component of the velocity field vanishes at the interface according to boundary condition (21). Thus, the surfactant evolution equation (35) can conveniently be analyzed by projecting the interfacial velocity onto the tangential vector harmonics

$$\mathbf{S}_{lm0} = [l(l+1)]^{-1/2}r\nabla_s Y_{lm}, \tag{67}$$

$$\mathbf{S}_{lm1} = \hat{\mathbf{r}} \times \mathbf{S}_{lm0}, \tag{68}$$

and the normal vector harmonics

$$\mathbf{S}_{lm2} = \hat{\mathbf{r}} Y_{lm}, \tag{69}$$

which form an orthonormal basis for vector fields on a unit sphere.

The matrix

$$\langle \mathbf{S}_{lmq} \delta_1 | \mathbf{v}_{l'm'q'}^\pm \rangle = \delta_{ll'} \delta_{mm'} \Psi_{qq'}^\pm(l), \tag{70}$$

with $\Psi_{qq'}^\pm(l)$ given by Eqs. (A.26) and (A.27), defines the transformation between representations (55) and (56) of the hydrodynamic operators $\hat{\mathbf{X}}$ and $\hat{\mathbf{W}}$, and the representations

$$\langle \mathbf{S}_{lmq} \delta_1 | 1 + \hat{\mathbf{X}} | \mathbf{v}_{l'm'q'}^+ \rangle = \delta_{ll'} \delta_{mm'} \bar{X}_{qq'}(l), \tag{71}$$

and

$$\langle \mathbf{S}_{lmq} \delta_1 | \hat{\mathbf{W}} | Y_{l'm'} \rangle = \delta_{ll'} \delta_{mm'} \bar{W}_{q'}(l). \tag{72}$$

Accordingly,

$$\bar{X}_{qq'}(l) = \Psi_{qq'}^+(l) + \Psi_{qq''}^-(l) X_{q''q'}(l) \tag{73}$$

and

$$\bar{W}_{q'}(l) = \Psi_{qq'}^-(l) W_{q'}(l), \tag{74}$$

which, combined with Eqs. (A.26), (A.27), (C.1), (C.15), yield

$$\bar{X}_{qq'}(l) = [l(l+1)]^{1/2} \begin{bmatrix} \frac{2l-1}{(l+1)\lambda_1} & 0 & \frac{(2l+1)(2l+3)}{2l\lambda_1} \\ 0 & \frac{2l+1}{3+(l-1)\lambda_1} & 0 \\ 0 & 0 & 0 \end{bmatrix} \quad (75)$$

and

$$\bar{W}_q(l) = \left[-\frac{[l(l+1)]^{1/2}}{(2l+1)\lambda_1}, 0, 0 \right], \quad (76)$$

where λ_1 is defined by Eq. (16). The matrix elements $\bar{X}_{2q}(l)$ and $\bar{W}_2(l)$ vanish because of boundary condition (21); $\bar{W}_1(l)$ vanishes because $\nabla_s Y_{lm}$ and S_{lm1} have different parity.

In this notation, the surfactant evolution equation (35) becomes

$$\begin{aligned} \frac{\partial \gamma_{lm}}{\partial t} = & -\langle Y_{lm} \delta_1 | \nabla_s | \mathbf{S}_{l'm'0} \rangle [\langle \mathbf{S}_{l'm'0} \delta_1 | 1 + \widehat{\mathbf{X}} | \mathbf{v}_{l''m''q}^+ \rangle c_{l''m''q}^+ \\ & + \langle \mathbf{S}_{l'm'0} \delta_1 | \bar{\Gamma} \mathbf{S}_{l''m''0} \rangle \langle \mathbf{S}_{l''m''0} \delta_1 | 1 + \widehat{\mathbf{X}} | \mathbf{v}_{l''m''m''q}^+ \rangle c_{l''m''m''q}^+ \\ & + \langle \mathbf{S}_{l'm'0} \delta_1 | \bar{\Gamma} \mathbf{S}_{l''m''1} \rangle \langle \mathbf{S}_{l''m''1} \delta_1 | 1 + \widehat{\mathbf{X}} | \mathbf{v}_{l''m''m''q}^+ \rangle c_{l''m''m''q}^+ \\ & + Ma \langle \mathbf{S}_{l'm'0} \delta_1 | \widehat{\mathbf{W}} | Y_{l''m''} \rangle \gamma_{l''m''} \\ & + Ma \langle \mathbf{S}_{l'm'0} \delta_1 | \bar{\Gamma} \mathbf{S}_{l''m''0} \rangle \langle \mathbf{S}_{l''m''0} \delta_1 | \widehat{\mathbf{W}} | Y_{l''m''} \rangle \gamma_{l''m''}], \end{aligned} \quad (77)$$

where Eqs. (38), (45), and

$$\langle Y_{lm} \delta_1 | \nabla_s | \mathbf{S}_{l'm'1} \rangle \equiv \langle Y_{lm} \delta_1 | \nabla_s \cdot \mathbf{S}_{l'm'1} \rangle = 0 \quad (78)$$

have been applied. The matrix elements of the surface-divergence operator are

$$\langle Y_{lm} \delta_1 | \nabla_s | \mathbf{S}_{l'm'0} \rangle = -[l(l+1)]^{1/2} \delta_{ll'} \delta_{mm'}, \quad (79)$$

which follows from definition (67). Eq. (38) gives

$$\langle \mathbf{S}_{lm0} \delta_1 | \bar{\Gamma} \mathbf{S}_{l'm'q} \rangle = \langle \mathbf{S}_{lm0} \delta_1 | Y_{l''m''} \mathbf{S}_{l'm'q} \rangle \gamma_{l''m''}, \quad q = 0, 1, \quad (80)$$

where $\langle \mathbf{S}_{lmq} \delta_1 | Y_{l''m''} \mathbf{S}_{l'm'q'} \rangle$ are the coupling coefficients between vector and scalar spherical harmonics, discussed in Appendix D.

Inserting Eqs. (71), (72), (79), and (80) into Eq. (77) yields

$$\begin{aligned} [l(l+1)]^{-1/2} \frac{\partial \gamma_{lm}}{\partial t} = & \bar{X}_{0q}(l) c_{lmq}^+ \\ & + [\langle \mathbf{S}_{lm0} \delta_1 | Y_{l''m''} \mathbf{S}_{l'm'0} \rangle \bar{X}_{0q}(l'') + \langle \mathbf{S}_{lm0} \delta_1 | Y_{l''m''} \mathbf{S}_{l'm'1} \rangle \bar{X}_{1q}(l'')] \gamma_{l''m''} c_{l''m''q}^+ \\ & + Ma \bar{W}_0(l) \gamma_{lm} + Ma \langle \mathbf{S}_{lm0} \delta_1 | Y_{l''m''} \mathbf{S}_{l'm'0} \rangle \bar{W}_0(l'') \gamma_{l''m''} \gamma_{l'm'}. \end{aligned} \quad (81)$$

This is the matrix equation for the surfactant distribution γ_{lm} ; all other quantities are known from Eqs. (62), (75), (76), (D.3), and (D.4). The equation is nondiagonal in quantum numbers l and m , because the coupling coefficients (D.3) and (D.4) are nondiagonal.

5. Perturbation analyses

In this section we derive perturbation expansions for the behavior of the system in three regimes: high Marangoni numbers (Section 5.1), high drop viscosities (Section 5.2), and low Marangoni numbers (Section 5.3). Explicit solutions are given for stationary shear flow (13).

5.1. Large Marangoni numbers

An analysis of the surfactant evolution equation (35) indicates that $\tilde{\Gamma} = O(Ma^{-1})$ for large Marangoni numbers. By rescaling

$$\tilde{\Gamma} = Ma^{-1} \tilde{\Gamma}^*, \tag{82}$$

Eq. (35) is transformed into

$$Ma^{-1} \frac{\partial \tilde{\Gamma}^*}{\partial t} = -\nabla_s \cdot [(1 + \hat{\mathbf{X}})\mathbf{u}_\infty + \hat{\mathbf{W}}\tilde{\Gamma}^*] - Ma^{-1} \nabla_s \cdot [\tilde{\Gamma}^*(1 + \hat{\mathbf{X}})\mathbf{u}_\infty + \tilde{\Gamma}^*\hat{\mathbf{W}}\tilde{\Gamma}^*], \tag{83}$$

which can be solved by a regular perturbation in Ma^{-1} . The perturbation expansion of (83) depends on the time scale for changes of surfactant concentration. In this paper we focus on the stationary behavior of the system; the time-dependent solution will be analyzed elsewhere [20].

The perturbation equations are constructed by inserting the expansion

$$\tilde{\Gamma}^* = \sum_{i=0}^{\infty} Ma^{-i} \tilde{\Gamma}^{(i)} \tag{84}$$

into the stationary form of Eq. (83), and collecting terms of the same order in Ma^{-1} . The following hierarchy of equations for $\tilde{\Gamma}^{(i)}$ is thus obtained

$$\nabla_s \cdot \hat{\mathbf{W}}\tilde{\Gamma}^{(i)} = -\nabla_s \cdot \left[\tilde{\Gamma}^{(i-1)}(1 + \hat{\mathbf{X}})\mathbf{u}_\infty + \sum_{k=0}^{i-1} \tilde{\Gamma}^{(k)}\hat{\mathbf{W}}\tilde{\Gamma}^{(i-1-k)} \right], \tag{85}$$

where $i = 0, 1, \dots$, and $\tilde{\Gamma}^{(-1)} = 1$.

Eq. (85) with $i = 0$ indicates that

$$\nabla_s \cdot \mathbf{u}^{(0)}(\hat{\mathbf{r}}) = 0, \tag{86}$$

where

$$\mathbf{u}^{(0)} = (1 + \hat{\mathbf{X}})\mathbf{u}_\infty + \hat{\mathbf{W}}\tilde{\Gamma}^{(0)} \tag{87}$$

is the interfacial velocity field for $Ma \rightarrow \infty$. Accordingly, the surface flow becomes incompressible [9]. For linear external flows (6), relation (86) implies that the drop undergoes rigid-body rotation

$$\mathbf{u}_s^{(0)} = \boldsymbol{\Omega} \times \hat{\mathbf{r}} \tag{88}$$

at high Marangoni numbers.

Using an analysis similar to that presented in Section 4, Eq. (85) can be transformed into the matrix representation, and then solved iteratively. The resulting solution is

$$\tilde{\gamma}_{lm}^{(0)} = -\bar{W}_0^{-1}(l)\bar{X}_{0q}(l)c_{lmq}^+ \quad (89)$$

for the leading-order term, and

$$\begin{aligned} \tilde{\gamma}_{lm}^{(i)} = & -\bar{W}_0^{-1}(l) \\ & \times \left\{ [\langle \mathbf{S}_{lm0}\delta_1 | Y_{l''m''}\mathbf{S}_{l'm'0} \rangle \bar{X}_{0q}(l') + \langle \mathbf{S}_{lm0}\delta_1 | Y_{l''m''}\mathbf{S}_{l'm'1} \rangle \bar{X}_{1q}(l')] \tilde{\gamma}_{l''m''}^{(i-1)} c_{l'm'q}^+ \right. \\ & \left. + \sum_{k=0}^{i-1} \langle \mathbf{S}_{lm0}\delta_1 | Y_{l''m''}\mathbf{S}_{l'm'0} \rangle \bar{W}_0(l') \tilde{\gamma}_{l''m''}^{(k)} \tilde{\gamma}_{l'm'}^{(i-1-k)} \right\}, \quad (90) \end{aligned}$$

for $i \geq 1$, where

$$\tilde{\gamma}_{lm}^{(i)} = \langle Y_{lm}\delta_1 | \tilde{I}^{(i)} \rangle. \quad (91)$$

Eqs. (89) and (90) are valid for arbitrary external flows.

For shear flow (62), the explicit solution was found by evaluating successive terms from the hierarchy (89) and (90). By this procedure, the first three terms in expansion (84) are

$$\tilde{I}^{(0)} = -i\left(\frac{5}{6}\right)^{1/2}\pi^{1/2}(Y_{22} - Y_{2-2}), \quad (92)$$

$$\tilde{I}^{(1)} = \left(\frac{5}{6}\right)^{3/2}\pi^{1/2}\lambda_1(Y_{22} + Y_{2-2}), \quad (93)$$

$$\tilde{I}^{(2)} = i\left(\frac{5}{6}\right)^{5/2}\pi^{1/2}\lambda_1^2(Y_{22} - Y_{2-2}) + i\frac{5}{8}\left(\frac{5}{14}\right)^{1/2}\pi^{1/2}\lambda_1(Y_{44} - Y_{4-4}), \quad (94)$$

where λ_1 is given by Eq. (16). Since the drop undergoes rigid-body rotation (88) at $Ma^{-1} = 0$, only the second term in the square brackets in Eq. (90) contributes to $\tilde{I}^{(1)}$.

As a consequence of Eqs. (62), (D.9), and (D.12), all coefficients $\gamma_{lm}^{(i)}$ with odd quantum numbers l and m vanish. The invariance of the system under the transformation $(x, y, z) \rightarrow (-x, y, -z)$ and $t \rightarrow -t$ (reversing the flow direction twice) implies

$$\gamma_{lm}^{(i)} = (-1)^{i+1}\gamma_{l-m}^{(i)}. \quad (95)$$

According to (D.10), the coupling of harmonics with orders l' and l'' produces only harmonics of orders $l \leq l' + l''$. Therefore,

$$\gamma_{lm}^{(i)} = 0 \quad \text{for } l > 2i, \quad i > 0, \quad (96)$$

and at each order the perturbative solution involves only finite matrices.

After the coefficients $\gamma_{lm}^{(i)}$ have been evaluated, the expansions for the surfactant contributions to the shear stress and normal stress differences,

$$\tau_{12}^{\Gamma} = \sum_{k=0}^{\infty} Ma^{-2k} \tau_{12}^{(2k)}, \tag{97}$$

$$N_i = \sum_{k=0}^{\infty} Ma^{-(2k+1)} N_i^{(2k+1)}, \quad i = 1, 2, \tag{98}$$

are obtained using (51), (53), (64)–(66), and (C.15). Only even powers of Ma^{-1} contribute to τ_{12}^{Γ} and odd powers of Ma^{-1} contribute to N_i , because the shear stress changes sign and the normal stresses are invariant under the transformation $(x, y, z) \rightarrow (-x, y, -z)$. Analytical expressions for first several terms in the expansions (97) and (98) are

$$\tau_{12}^{(0)} = \frac{3}{2} \lambda_1^{-1}, \tag{99}$$

$$\tau_{12}^{(2)} = -\frac{3}{2} \left(\frac{5}{6}\right)^2 \lambda_1, \tag{100}$$

$$\tau_{12}^{(4)} = \frac{3}{2} \left(\frac{5}{6}\right)^4 \lambda_1^3 \left(1 - \frac{19}{14} \lambda_1^{-2}\right), \tag{101}$$

$$\tau_{12}^{(6)} = -\frac{3}{2} \left(\frac{5}{6}\right)^6 \lambda_1^5 \left(1 - \frac{59\,961}{8\,750} \lambda_1^{-2} + \frac{34\,157\,611}{15\,415\,400} \lambda_1^{-4}\right), \tag{102}$$

$$N_1^{(1)} = \frac{5}{2}, \tag{103}$$

$$N_1^{(3)} = -\frac{5}{2} \left(\frac{5}{6}\right)^2 \lambda_1^2 \left(1 - \frac{5}{14} \lambda_1^{-2}\right), \tag{104}$$

$$N_1^{(5)} = \frac{5}{2} \left(\frac{5}{6}\right)^4 \lambda_1^4 \left(1 - \frac{1193}{350} \lambda_1^{-2} + \frac{11\,859}{40\,040} \lambda_1^{-4}\right), \tag{105}$$

$$N_2^{(1)} = -\frac{1}{2} N_1^{(1)}, \tag{106}$$

$$N_2^{(3)} = -\frac{1}{2} N_1^{(3)}, \tag{107}$$

$$N_2^{(5)} = -\frac{1}{2} N_1^{(5)} + \frac{22\,375}{118\,272} \lambda_1. \tag{108}$$

The Einstein result

$$\tau_{12}^d = \frac{5}{2} \tag{109}$$

is recovered from Eqs. (15) and (99), because the drop behaves as a rigid particle for $Ma^{-1} \rightarrow 0$.

As shown in the following subsection (cf. Eq. (124)), the radius of convergence for the expansions (84), (97), and (98) is

$$Ma^{-1} = \lambda_1^{-1}. \tag{110}$$

5.2. High viscosity drops

For a freely rotating drop, the rotational component (8) of the external flow does not generate a scattered flow. Therefore,

$$(1 + \widehat{\mathbf{X}})\mathbf{u}_\infty^r = \mathbf{u}_\infty^r, \quad (111)$$

which follows from Eqs. (60) and (C.1). The flow fields $(1 + \widehat{\mathbf{X}})\mathbf{u}_\infty^s$ and $\widehat{\mathbf{W}}\bar{\Gamma}$ are associated with nonrigid circulation of the fluid in the drop; thus, these contributions scale with the viscosity ratio. Eqs. (71), (72), and (75), (76) indicate that the following scalings are appropriate

$$\widehat{\mathbf{X}}' = \lambda_1(1 + \widehat{\mathbf{X}})\widehat{\mathbf{P}} \quad (112)$$

and

$$\widehat{\mathbf{W}}' = \lambda_1\widehat{\mathbf{W}}, \quad (113)$$

where $\widehat{\mathbf{P}}$ is the projection operator onto the subspace $\{q=0,2\}$ in the surface representation (67)–(69) (thus $\widehat{\mathbf{P}}\mathbf{u}_\infty = \mathbf{u}_\infty^s$), and the operators $\widehat{\mathbf{X}}'$ and $\widehat{\mathbf{W}}'$ are independent of λ . Inserting (111)–(113) into Eq. (35) yields

$$\begin{aligned} \frac{\partial \Gamma'}{\partial t} + \nabla_s \cdot (\mathbf{u}_\infty^r \Gamma' + \tilde{M}a \widehat{\mathbf{W}}' \Gamma') \\ = -\nabla_s \cdot \widehat{\mathbf{X}}' \mathbf{u}_\infty^s - \lambda_1^{-1} \nabla_s \cdot (\Gamma' \widehat{\mathbf{X}}' \mathbf{u}_\infty^s + \tilde{M}a \Gamma' \widehat{\mathbf{W}}' \Gamma'), \end{aligned} \quad (114)$$

where both surfactant concentration and Marangoni number are rescaled,

$$\Gamma' = \lambda_1 \bar{\Gamma}, \quad (115)$$

$$\tilde{M}a = \lambda_1^{-1} Ma. \quad (116)$$

The perturbation equations are constructed by inserting the expansion

$$\Gamma' = \sum_{i=0}^{\infty} \lambda_1^{-i} \Gamma'^{(i)} \quad (117)$$

into (114), and collecting terms of the same order in λ_1^{-1} . The resulting hierarchy equations are

$$\begin{aligned} \frac{\partial \Gamma'^{(i)}}{\partial t} + \nabla_s \cdot (\mathbf{u}_\infty^r \Gamma'^{(i)} + \tilde{M}a \widehat{\mathbf{W}}' \Gamma'^{(i)}) \\ = -\nabla_s \cdot (\Gamma'^{(i-1)} \widehat{\mathbf{X}}' \mathbf{u}_\infty^s + \sum_{k=0}^{i-1} \tilde{M}a \Gamma'^{(k)} \widehat{\mathbf{W}}' \Gamma'^{(i-1-k)}), \end{aligned} \quad (118)$$

where $i = 0, 1, \dots$, and $\Gamma'^{(-1)} = 1$. The high-viscosity expansion (117) is uniformly valid for all Ma , because the second term on the left-hand side of Eq. (114) always dominates the right-hand side.

By the procedure described in Section 4, hierarchy (118) can be cast in matrix form. For stationary shear flow (62), this yields

$$\gamma'_{lm}{}^{(0)} = -[\langle \mathbf{S}_{lm0} \delta_1 | Y_{lm} \mathbf{S}_{101} \rangle \bar{X}_{11}(1) c_{101}^+ + \tilde{M} a W'_0(l)]^{-1} X'_{0q}(l) c_{lmq}^+ \tag{119}$$

for the leading-order term, and

$$\begin{aligned} \gamma'_{lm}{}^{(i)} = & -[\langle \mathbf{S}_{lm0} \delta_1 | Y_{lm} \mathbf{S}_{101} \rangle \bar{X}_{11}(1) c_{101}^+ + \tilde{M} a W'_0(l)]^{-1} \langle \mathbf{S}_{lm0} \delta_1 | Y_{l'm''} \mathbf{S}_{l'm'0} \rangle \\ & \times \left[X'_{0q}(l') \gamma'_{l'm''}{}^{(i-1)} c_{l'm'q}^+ + \tilde{M} a W'_0(l') \sum_{k=0}^{i-1} \gamma'_{l'm''}{}^k \gamma'_{l'm'}{}^{i-1-k} \right] \end{aligned} \tag{120}$$

for $i \geq 1$, where

$$\gamma'_{lm}{}^{(i)} = \langle Y_{lm} \delta_1 | \Gamma'^{(i)} \rangle, \tag{121}$$

$$X'_{0q} = \lambda_1 \bar{X}_{0q}, \tag{122}$$

$$W'_q = \lambda_1 \bar{W}_q, \tag{123}$$

and the matrix element $\langle \mathbf{S}_{lm0} \delta_1 | Y_{lm} \mathbf{S}_{101} \rangle$ is given by Eq. (D.13).

From Eqs. (62), (75), (76), (D.13) and the form of Eqs. (119) and (120), it follows that the expansion coefficients $\Gamma'^{(i)}$ have poles in the complex inverse-Marangoni-number plane at

$$\tilde{M} a^{-1} = \pm i \frac{2l(l+1)}{m(2l+1)}, \tag{124}$$

where $l \geq 2$, $2 \leq m \leq l$, and both l and m are even. Set (124) is dense on the lines $\tilde{M} a^{-1} = iy$ for $|y| > 1$, which indicates that $\bar{\Gamma}$ has branch-cuts on these lines. This result indicates that the radius of convergence for the large-Marangoni-number expansions presented in Section 5.1 is given by Eq. (110).

After the coefficients $\gamma'_{lm}{}^{(i)}$ have been evaluated, the expansions for the surfactant contribution to shear stress and normal stress differences are obtained using (51), (53), (64)–(66), and (C.15),

$$\tau_{12}^{\Gamma} = \sum_{k=0}^{\infty} \lambda_1^{-(2k+1)} \tau_{12}'^{(2k+1)}, \tag{125}$$

$$N_1 = \sum_{k=0}^{\infty} \lambda_1^{-(2k+1)} N_1'^{(2k+1)}, \tag{126}$$

$$N_2 = -\frac{1}{2} N_1 + \sum_{k=2}^{\infty} \lambda_1^{-2k} N_2'^{(2k)}, \tag{127}$$

where $\tau_{12}'^{(m)}$ and $N_i'^{(m)}$ are functions of $\tilde{M} a$. Only odd powers of λ_1^{-1} contribute to τ_{12}^{Γ} and N_1 ; the second normal stress difference N_2 depends on both odd and even powers

of λ_1^{-1} . Analytical expressions for first few terms in expansions (125)–(127) are

$$\tau'_{12}{}^{(1)} = \frac{3}{2} \frac{1}{1 + (\frac{5}{6})^2 \tilde{M}a^{-2}}, \quad (128)$$

$$\tau'_{12}{}^{(3)} = -\frac{3}{2} \left(\frac{5}{6}\right)^4 \frac{19}{14} \frac{\tilde{M}a^{-4} (1 - \frac{233}{380} \tilde{M}a^{-2})}{[1 + (\frac{5}{6})^2 \tilde{M}a^{-2}]^3 [1 + (\frac{9}{10})^2 \tilde{M}a^{-2}]}, \quad (129)$$

$$N_1^{(1)} = \frac{5}{2} \frac{\tilde{M}a^{-1}}{[1 + (\frac{5}{6})^2 \tilde{M}a^{-2}]}, \quad (130)$$

$$N_1^{(3)} = 3 \left(\frac{5}{6}\right)^3 \frac{5}{14} \frac{\tilde{M}a^{-3} (1 - \frac{6722}{1800} \tilde{M}a^{-2} + \frac{675}{1800} \tilde{M}a^{-4})}{[1 + (\frac{5}{6})^2 \tilde{M}a^{-2}]^3 [1 + (\frac{9}{10})^2 \tilde{M}a^{-2}]}, \quad (131)$$

and

$$N_2^{(4)} = \frac{22\,375}{118\,272} \frac{\tilde{M}a^{-5} (1 + \frac{2349}{17\,900} \tilde{M}a^{-2})}{[1 + (\frac{5}{6})^2 \tilde{M}a^{-2}]^2 [1 + (\frac{9}{10})^2 \tilde{M}a^{-2}] [1 + (\frac{9}{20})^2 \tilde{M}a^{-2}]}. \quad (132)$$

Several additional terms are listed in Appendix E. The Einstein result (109) is recovered from Eqs. (15) and (128) for $Ma^{-1} \rightarrow 0$. As shown in Appendix F.2, the $O(\lambda_1^{-1})$ terms in expansions (125)–(127) are equivalent to the solution of Eq. (81) with all matrices truncated at the level $l = 2$.

The expansion coefficients $\tau'_{12}{}^{(2k+1)}$, $N_1^{(2k+1)}$, and $N_2^{(2k)}$ with $k \leq 4$ are plotted in Fig. 1 as functions of $\tilde{M}a^{-1}$. The results indicate that the magnitude of the coefficients decreases with increasing k ; thus, expansions (125)–(127) converge for all $\lambda > 0$. Further discussion of the high-viscosity-expansion results is given in Section 7.

5.3. Small Marangoni numbers

In the high-shear-rate limit, surfactant is passively convected on the drop interface. For $Ma \rightarrow 0$, the evolution equation (35) reduces to

$$\frac{\partial \bar{\Gamma}}{\partial t} = -(\nabla_s \cdot \Gamma \mathbf{u}_0), \quad (133)$$

where

$$\mathbf{u}_0 = (1 + \hat{\mathbf{X}}) \mathbf{u}_\infty \quad (134)$$

is the velocity field for a drop with clean interface in the external flow.

Stationary solutions of Eq. (133) were obtained by the method of characteristics, as shown in Section F.1 of Appendix F; the nonsingular stationary surfactant distribution for two-dimensional external linear flows (6) with

$$E_{ij} = \frac{1}{2} [(1 + \alpha) \delta_{i1} \delta_{j2} + (1 - \alpha) \delta_{i2} \delta_{1j}] \quad (135)$$

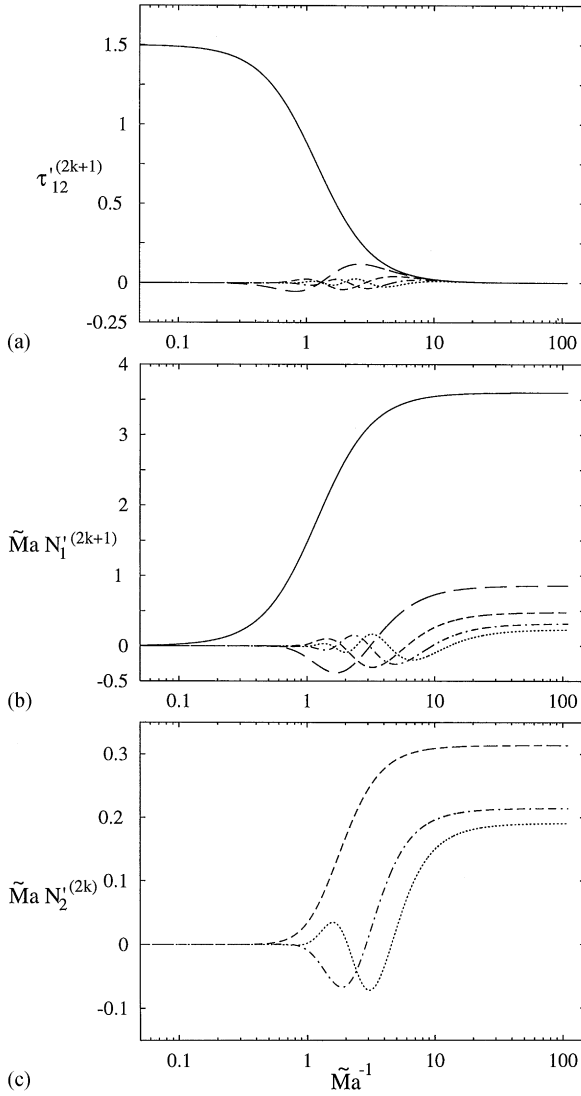


Fig. 1. High-viscosity-expansion coefficients for (a) shear stress, (b) first normal stress difference, and (c) second normal stress difference, as a functions of rescaled inverse Marangoni number. The results for $k = 0$ (solid lines); $k = 1$ (long-dashed lines); $k = 2$ (dashed lines); $k = 3$ (dash-dotted lines); $k = 4$ (dotted lines).

is

$$\Gamma(\theta, \varphi) = g(\theta_0) \left\{ \frac{\lambda_1 \alpha + 1}{\lambda_1 \alpha + 1 - \sin^2 \theta [\cos(2\varphi) + 1]} \right\}^{3/2}, \tag{136}$$

where θ, φ are the spherical coordinates,

$$\theta_0(\varphi) = \arctan \left[\left(\frac{\lambda_1 \alpha - \cos 2\varphi}{\lambda_1 \alpha + 1} \right)^{1/2} \tan \theta \right], \tag{137}$$

and $g(\theta_0) \geq 0$ is an arbitrary function. Eq. (136) is valid, provided that

$$\lambda_1 > \alpha^{-1}. \quad (138)$$

For shear flow ($\alpha = 1$), this condition is satisfied for $\lambda \neq 0$. For linear flows with less rotation ($\alpha < 1$) condition (138) is violated at low viscosity ratios; under these conditions surfactant free regions and singular points occur on the drop interface.

The symmetry

$$\Gamma(\theta, \varphi) = \Gamma(\theta, -\varphi) \quad (139)$$

of solution (136) (corresponding to flow reversal) implies the following behavior of shear and normal stresses normalized by characteristic Marangoni stresses $\Delta\sigma/a$:

$$\lim_{Ma \rightarrow 0} Ma^{-1} \tau_{12}^{\Gamma} = 0, \quad (140)$$

$$\lim_{Ma \rightarrow 0} Ma^{-1} N_i \neq 0, \quad i = 1, 2. \quad (141)$$

According to (136), the stationary surfactant distribution is nonunique for $Ma = 0$. For small, but finite Marangoni numbers a slow drift of surfactant occurs across the clean-drop streamlines, and distribution (136) slowly evolves towards a unique stationary state. To find this stationary state, the full nonlinear problem (35) needs to be solved.

Eq. (35) can be analyzed by a regular perturbation in Ma . Expanding

$$\bar{\Gamma} = \sum_{i=0}^{\infty} Ma^i \bar{\Gamma}^{(i)}, \quad (142)$$

and using a procedure similar to that described in Section 5.1, yields a hierarchy of perturbation equations for

$$\bar{\gamma}_{lm}^{(i)} = \langle Y_{lm} \delta_1 | \bar{\Gamma}^{(i)} \rangle. \quad (143)$$

For the stationary problem, the leading-order equation is

$$A_{lm'l'm'} \gamma_{l'm'}^{(0)} = -\bar{X}_{0q}(l) c_{lmq}^+, \quad (144)$$

and

$$A_{lm'l'm'} \gamma_{l'm'}^{(i)} = -\bar{W}_0(l) \gamma_{lm}^{(i-1)} - \sum_{k=0}^{i-1} \langle \mathbf{S}_{lm0} \delta_1 | Y_{l'm''} \mathbf{S}_{l'm''q} \rangle \bar{W}_0(l') \gamma_{l'm''}^k \gamma_{l'm'}^{i-1-k} \quad (145)$$

for $i \geq 1$, where

$$A_{lm'l'm'} = \langle \mathbf{S}_{lm0} \delta_1 | Y_{l'm'} \mathbf{S}_{l'm''q} \rangle \bar{X}_{qq''}(l'') c_{l'm''q''}^+. \quad (146)$$

Since the matrix $A_{lm'l'm'}$ is non-diagonal, the iterative solution of (144) and (145) involves, at each order i , nonzero coefficients $\gamma_{lm}^{(i)}$ with arbitrarily large l and m , unlike Eqs. (89) and (90).

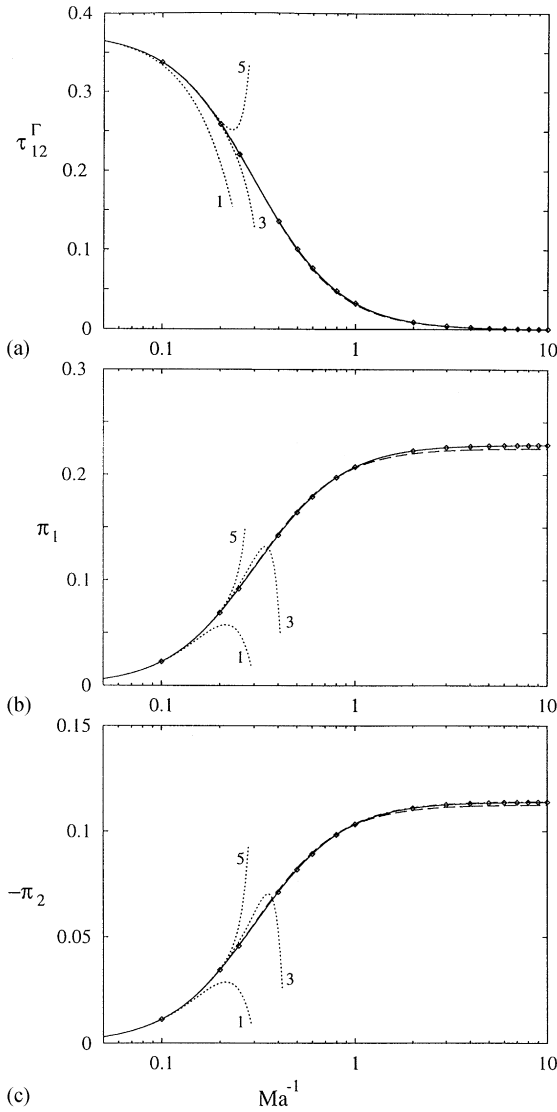


Fig. 2. Viscosity coefficient (a) and first (b) and second (c) normal stress differences as a functions of inverse Marangoni number, for viscosity ratio $\lambda=3$. Numerical solution of Eq. (81) (points); high-Marangoni number expansions (97) and (98) truncated at k as labeled (dotted lines); large λ expansions (125)–(127), truncated at $O(\lambda_1^{-1})$ (dashed line), at $O(\lambda_1^{-3})$ (dot-dashed line), at $O(\lambda_1^{-5})$ (solid line). Note that the $O(\lambda_1^{-3})$ and $O(\lambda_1^{-5})$ curves coincide; on (a) the $O(\lambda_1^{-1})$ result is indistinguishable from the higher-order results.

The discussion presented in Section F.2 of Appendix F indicates that, for shear flow, the matrix $A_{lm'l'm'}$ is singular, and Eq. (144) has an infinite family of solutions (which is consistent with the nonuniqueness of (136)). The unique solution $\gamma_{lm}^{(0)}$ corresponding

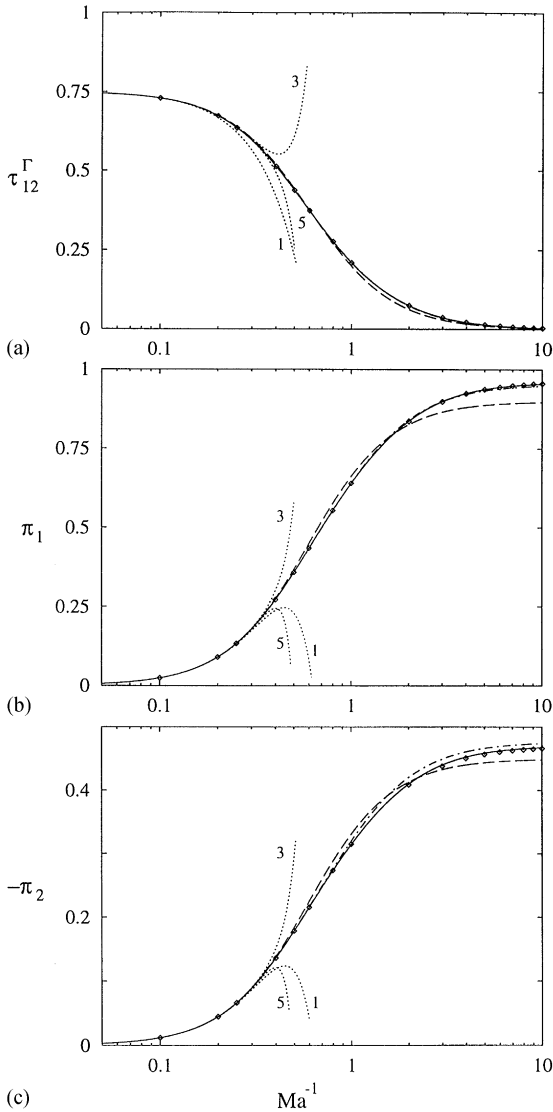


Fig. 3. Same as in Fig. 2 for viscosity ratio $\lambda = 1$. The $O(\lambda_1^{-3})$ and $O(\lambda_1^{-5})$ curves coincide in (a) and (b).

to finite Ma is chosen by the existence condition for $\gamma_{lm}^{(1)}$. Further analysis of Eqs. (144) and (145) is presented in Appendix F.2.

6. Numerical solution

Eq. (81) was also solved by time integration from the initial condition $\gamma_{lm} = 0$ at $t = 0$ until a stationary state was achieved. The infinite set of evolution equations was

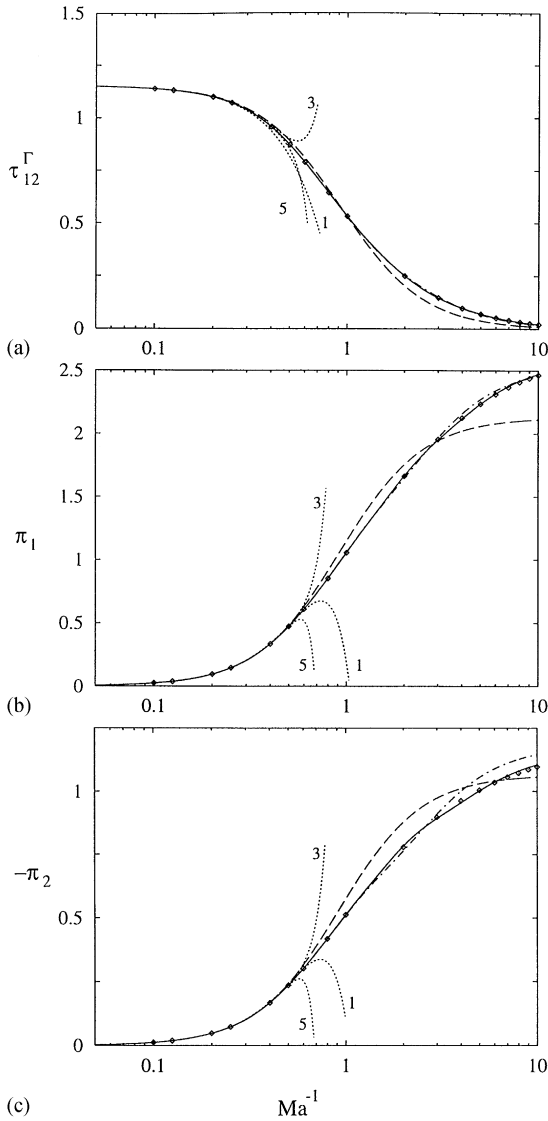


Fig. 4. Same as in Fig. 2 for viscosity ratio $\lambda=0.3$, except that large λ expansions (125)–(127) are truncated at $O(\lambda_1^{-1})$ (dashed line), at $O(\lambda_1^{-5})$ (dot-dashed line), at $O(\lambda_1^{-9})$ (solid line). The $O(\lambda_1^{-5})$ and $O(\lambda_1^{-9})$ curves coincide in (a).

truncated by setting $\gamma_{lm} = 0$ for $l > l_{\max}$, where $l_{\max} \leq 12$ was used. The surfactant contribution to the stress is obtained to within several percent using $l_{\max} = 2$ for calculations with $\lambda = 3$. Larger values are needed at low viscosities; for $\lambda = 0.3$, accurate results require $l_{\max} = 8$.

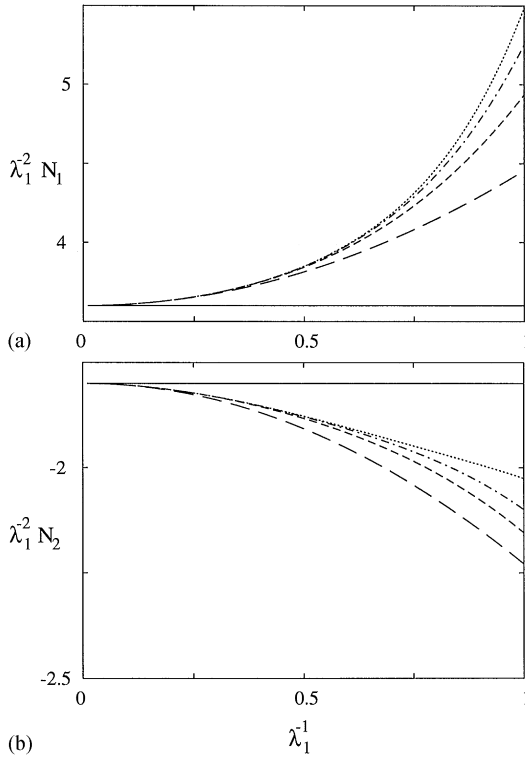


Fig. 5. High-shear-rate limit ($Ma^{-1} \rightarrow \infty$) of the first (a) and second (b) normal stress differences (normalized by Marangoni stresses) as functions of $\hat{\lambda}_1^{-1}$. Results from high-viscosity expansions (126) and (127) truncated at $k = 1$ (solid lines); $k = 2$ (long-dashed lines); $k = 3$ (dashed lines); $k = 4$ (dash-dotted lines); $k = 5$ (dotted lines).

7. Discussion

The surfactant contribution to the shear stress and normal stress differences for a dilute emulsion in stationary shear flow are presented in Figs. 2–4 for three values of λ , as functions of Ma^{-1} (the dimensionless shear rate). Shear stresses are normalized by $\eta\dot{\gamma}$ thus, τ^F represents the modification of the emulsion shear viscosity by the presence of surfactant. The contributions to the normal stress differences

$$\pi_i = Ma^{-1} N_i, \quad i = 1, 2, \quad (147)$$

are normalized by the characteristic value of Marangoni stress $a^{-1} k_B T T_{eq}$. Figs. 2–4 in the appendix show results obtained from high-Marangoni-number expansion (97), and (98), high-viscosity expansion (125)–(127), and from numerical solution of Eq. (81).

The results show that surfactant effects are most significant for low-viscosity ratios. Shear thinning behavior is evident. The total drop contribution (14) to the shear viscosity decreases from the rigid particle value (109) at low shear rates to the value (15),

corresponding to a clean drop, at high shear rates; the transition occurs for $Ma^{-1} \approx \lambda_1^{-1}$. At high shear rates ($Ma^{-1} \rightarrow \infty$), the surfactant contribution to the shear stress τ^F vanishes as Ma^2 , and the normal stress contributions π_1, π_2 approach constant values. These observations agree with the analyses in Section 5. The limiting high-shear-rate values of π_1, π_2 calculated from the high-viscosity expansions (126) and (127) are shown in Fig. 5 as functions of λ_1^{-1} .

The results shown in Figs. 2–4 indicate that the high-viscosity expansion (125)–(127) converges rapidly, even for the lowest viscosity ratio shown. For $\lambda = 3$, the first term in the expansion is accurate to several percent. As discussed in Section 5.2, the high-viscosity expansion converges for all $\lambda > 0$; however, the results presented in Fig. 5 indicate that the convergence slows for low viscosity ratios. In the low-shear-rate regime $Ma^{-1} < \lambda_1^{-1}$, the high-viscosity expansion always converges rapidly.

The results of the low-shear-rate expansions (97) and (98) are consistent with the convergence radius (110).

8. Conclusions

This paper describes a theoretical study on the rheology of a diluted emulsion with surfactant-covered spherical drops. The system is characterized by the Marangoni number and drop viscosity. A matrix formulation was derived for the nonlinear single-drop problem of fluid motion and surfactant transport. Numerical solutions for the surfactant distribution and the rheological contribution of the drops were obtained by truncating the infinite set of equations. Analytical results were derived by perturbation expansions for low shear rates and for high-viscosity drops; the high-viscosity expansion converges rapidly over a broad range of parameters.

Our results show that the rheological contributions of the drops can be significantly affected by small quantities of surfactant. Shear thinning and nonzero normal stress differences are quantitatively predicted. In a forthcoming paper, the nonlinear frequency response of a diluted emulsion of surfactant-covered drops will be analyzed using the formalism developed herein [20].

At leading order, the effects of drop deformation and Marangoni stresses are additive. Thus, the leading-order results presented in this paper may be combined with existing small deformation theories [21,22]. It may be possible to generalize our theory to describe the higher-order coupled effects of surfactant redistribution and drop deformation. The single-particle solution presented here can be incorporated into an effective medium approximation or a cluster expansion theory for concentrated emulsions.

Acknowledgements

This work was supported by NSF grant CTS-9624615, NASA grant NAG3-1935, and a grant from the Whitaker Foundation.

Appendix A. Basic sets of solutions of Stokes equations

A.1. Representation in adjoined bases

For completeness, we list the basic sets of solutions \mathbf{v}_{lmq}^{\pm} and the orthonormal functions \mathbf{w}_{lmq}^{\pm} , introduced in Ref. [14].

The functions \mathbf{v}_{lmq}^{\pm} and \mathbf{w}_{lmq}^{\pm} are represented in terms of the normalized vector spherical harmonics [23]

$$\mathbf{Y}_{l|l-1m}(\hat{\mathbf{r}}) = a_l^{-1} r^{-l+1} \nabla[r^l Y_{lm}(\hat{\mathbf{r}})], \quad (\text{A.1})$$

$$\mathbf{Y}_{l|l+1m}(\hat{\mathbf{r}}) = b_l^{-1} r^{l+2} \nabla[r^{-(l+1)} Y_{lm}(\hat{\mathbf{r}})], \quad (\text{A.2})$$

$$\mathbf{Y}_{l|lm}(\hat{\mathbf{r}}) = c_l^{-1} \mathbf{r} \times \nabla_s Y_{lm}(\hat{\mathbf{r}}), \quad (\text{A.3})$$

where

$$Y_{lm}(\hat{\mathbf{r}}) = n_{lm}^{-1} (-1)^m P_l^m(\cos \theta) e^{im\varphi} \quad (\text{A.4})$$

are the normalized scalar spherical harmonics, and the normalization coefficients are

$$a_l = [l(2l+1)]^{1/2}, \quad (\text{A.5})$$

$$b_l = [(l+1)(2l+1)]^{1/2}, \quad (\text{A.6})$$

$$c_l = -i[l(l+1)]^{1/2}, \quad (\text{A.7})$$

$$n_{lm} = \left[\frac{4\pi}{2l+1} \frac{(l+m)!}{(l-m)!} \right]^{1/2}. \quad (\text{A.8})$$

The parity of the harmonics $\mathbf{Y}_{l|l'm}$ is $(-1)^{l'}$.

In Dirac notation, the expression for the basic functions $\mathbf{a}_{lmq}^{\pm}(\mathbf{r}) = \mathbf{v}_{lmq}^{\pm}(\mathbf{r})$, $\mathbf{w}_{lmq}^{\pm}(\mathbf{r})$ are

$$|\mathbf{a}_{lmq}^{\pm}\rangle = |\mathbf{Y}_{l|l-1+qm}\rangle \langle \mathbf{Y}_{l|l-1+qm} \delta_r | \mathbf{a}_{l'm'q'}^{\pm}\rangle. \quad (\text{A.9})$$

The matrix elements in Eq. (A.9) are diagonal in the quantum numbers l and m ; thus,

$$\langle \mathbf{Y}_{l|l-1+qm} \delta_r | \mathbf{v}_{l'm'q'}^{\pm}\rangle = \delta_{ll'} \delta_{mm'} V_{qq'}^{\pm}(l; r), \quad (\text{A.10})$$

and

$$\langle \mathbf{Y}_{l|l-1+qm} \delta_r | \mathbf{w}_{l'm'q'}^{\pm}\rangle = \delta_{ll'} \delta_{mm'} W_{qq'}^{\pm}(l; r). \quad (\text{A.11})$$

The explicit expressions for the matrices V^{\pm} and W^{\pm} are

$$V^+(l; r) = \begin{bmatrix} a_l r^{l-1} & 0 & \frac{(l+1)(2l+3)}{2l} a_l r^{l+1} \\ 0 & i c_l r^l & 0 \\ 0 & 0 & b_l r^{l+1} \end{bmatrix}, \quad (\text{A.12})$$

$$V^-(l; r) = (2l + 1)^{-2} \begin{bmatrix} \frac{l+1}{l(2l-1)} a_l r^{-l} & 0 & 0 \\ 0 & i \frac{2l+1}{l(l+1)} c_l r^{-(l+1)} & 0 \\ -\frac{1}{2} b_l r^{-l} & 0 & \frac{l}{(l+1)(2l+3)} b_l r^{-(l+2)} \end{bmatrix}, \tag{A.13}$$

and

$$W^+(l; r) = r^2 \begin{bmatrix} \frac{1}{l(2l+1)} a_l r^{-(l-1)} & 0 & 0 \\ 0 & i \frac{1}{l(l+1)} c_l r^{-l} & 0 \\ -\frac{2l+3}{2l(2l+1)} b_l r^{-(l-1)} & 0 & \frac{1}{(l+1)(2l+1)} b_l r^{-(l+1)} \end{bmatrix}, \tag{A.14}$$

$$W^-(l; r) = (2l + 1)r^2 \begin{bmatrix} \frac{2l-1}{l+1} a_l r^l & 0 & \frac{(2l-1)(2l+3)}{2l} a_l r^{l+2} \\ 0 & i c_l r^{l+1} & 0 \\ 0 & 0 & \frac{2l+3}{l} b_l r^{l+2} \end{bmatrix}. \tag{A.15}$$

The flow fields \mathbf{v}_{lmq}^+ with $l = 1, 2, \dots$, $m = -l, \dots, l$, and $q = 0, 1, 2$ form a complete set of nonsingular fundamental solutions of Stokes equations, and \mathbf{v}_{lmq}^- a complete set of solutions that vanish at infinity. Only $\mathbf{v}_{lm2}^+(\mathbf{r})$ and $\mathbf{v}_{lm0}^-(\mathbf{r})$ are associated with nonzero pressure fields,

$$p_{lm2}^+(\mathbf{r}) = \frac{(l + 1)(2l + 1)(2l + 3)}{l} r^l Y_{lm}(\hat{\mathbf{r}}), \tag{A.16}$$

$$p_{lm0}^-(\mathbf{r}) = \frac{1}{2l + 1} r^{-(l+1)} Y_{lm}(\hat{\mathbf{r}}). \tag{A.17}$$

The functions \mathbf{v}_{lmq}^\pm and \mathbf{w}_{lmq}^\pm satisfy the orthonormality conditions (43).

The normalization of the functions \mathbf{v}_{lmq}^\pm , \mathbf{w}_{lmq}^\pm defined above differs from that used by Cichocki, Felderhof, and Schmitz (CFS) [14]. The two sets of functions are related by

$$\mathbf{v}_{lmq}^\pm = n_{lm}^{-1} \mathbf{v}_{lmq}^{\pm\text{CFS}}, \tag{A.18}$$

$$\mathbf{w}_{lmq}^\pm = r n_{lm} \mathbf{w}_{lmq}^{\pm\text{CFS}}, \tag{A.19}$$

where n_{lm} is given by (A.8). Furthermore, delta function (41) in orthonormality condition (43) has an extra factor r^{-1} . In the present normalization, the matrix elements of isotropic operators are independent of m .

A.2. Representation in surface basis

The equation that describes the evolution of the surfactant distribution on the drop interface, and the boundary conditions for the fluid velocity require decomposition of the interfacial flow into tangential and normal components. Thus, expansions in tangential and normal vector harmonics (67)–(69) are appropriate for the analysis of

this problem. The transformation between the harmonics \mathbf{S}_{lmq} and $\mathbf{Y}_{l|l-1+qm}$ is given by the matrix

$$\langle \mathbf{S}_{lmq} \delta_1 | \mathbf{Y}_{l'l'-1+q'm'} \rangle = \delta_{ll'} \delta_{mm'} H_{qq'}(l), \quad (\text{A.20})$$

where

$$H_{qq'}(l) = \begin{bmatrix} \left(\frac{l+1}{2l+1}\right)^{1/2} & 0 & \left(\frac{l}{2l+1}\right)^{1/2} \\ 0 & 1 & 0 \\ \left(\frac{l}{2l+1}\right)^{1/2} & 0 & -\left(\frac{l+1}{2l+1}\right)^{1/2} \end{bmatrix}. \quad (\text{A.21})$$

Note that with the choice of basis, (67)–(69), $\det(H_{qq'}) = -1$, and

$$H_{qq'}^{-1} = H_{qq'}. \quad (\text{A.22})$$

We introduce the sets of basic Stokes-flow solutions that satisfy the boundary condition

$$\mathbf{u}_{lmq}^{\pm}(\mathbf{r}) = \mathbf{S}_{lmq}(\hat{\mathbf{r}}) \quad \text{at } r = 1. \quad (\text{A.23})$$

The solutions $\mathbf{u}_{lmq}^{+}(\mathbf{r})$ are nonsingular, and the solutions $\mathbf{u}_{lmq}^{-}(\mathbf{r})$ vanish at infinity. The linear relation

$$|\mathbf{v}_{lmq}^{\pm}\rangle = |\mathbf{u}_{lmq}^{\pm}\rangle \langle \mathbf{S}_{lmq} \delta_1 | \mathbf{v}_{l'm'q'}^{\pm}\rangle \quad (\text{A.24})$$

between fundamental solutions $\mathbf{u}_{lmq}^{\pm}(\mathbf{r})$ and $\mathbf{v}_{lmq}^{\pm}(\mathbf{r})$ is given by matrix (70), where

$$\Psi_{qq'}^{\pm}(l) = H_{qq''}(l) V_{q''q'}^{\pm}(l; 1). \quad (\text{A.25})$$

The explicit relation for the matrices $\Psi_{qq'}^{\pm}$ are

$$\Psi_{qq'}^{+}(l) = \begin{bmatrix} [l(l+1)]^{1/2} & 0 & \frac{1}{2} \left(\frac{l+1}{l}\right)^{1/2} (l+3)(2l+1) \\ 0 & [l(l+1)]^{1/2} & 0 \\ l & 0 & \frac{1}{2} (l+1)(2l+1) \end{bmatrix}, \quad (\text{A.26})$$

$$\Psi_{qq'}^{-}(l) = (2l+1)^{-1} \begin{bmatrix} -\left(\frac{l+1}{l}\right)^{1/2} \frac{l-2}{2(2l-1)} & 0 & \left(\frac{l}{l+1}\right)^{1/2} \frac{l}{(2l+1)(2l+3)} \\ 0 & [l(l+1)]^{-1/2} & 0 \\ \frac{l+1}{2(2l-1)} & 0 & -\frac{l}{(2l+1)(2l+3)} \end{bmatrix}. \quad (\text{A.27})$$

The expression for $\mathbf{u}_{lmq}^{\pm}(\mathbf{r})$ in terms of harmonics \mathbf{S}_{lmq} is

$$|\mathbf{u}_{lmq}^{\pm}\rangle = |\mathbf{S}_{lmq}^{\pm}\rangle \langle \mathbf{S}_{lmq} \delta_r | \mathbf{u}_{l'm'q'}^{\pm}\rangle, \quad (\text{A.28})$$

where

$$\langle \mathbf{S}_{lmq} \delta_r | \mathbf{u}_{l'm'q'}^{\pm}\rangle = \delta_{ll'} \delta_{mm'} U_{qq'}(l; r), \quad (\text{A.29})$$

and

$$U_{qq'}^{\pm}(l; r) = H_{qq''}(l) V_{q''q'}^{\pm}(l; r) [\Psi^{\pm}(l)]_{q''q'}^{-1}. \quad (\text{A.30})$$

Eqs. (A.12), (A.13), (A.21), and (A.26), (A.27) yield

$$U_{qq'}^+(l; r) = \frac{1}{2}r^{l-1} \begin{bmatrix} -(l+1) + (l+3)r^2 & 0 & (3+l)\left(\frac{l+1}{l}\right)^{1/2}(1-r^2) \\ 0 & 2r & 0 \\ -[l(1+l)]^{1/2}(1-r^2) & 0 & l+3 - (l+1)r^2 \end{bmatrix}, \tag{A.31}$$

$$U_{qq'}^-(l; r) = \frac{1}{2}r^{-l} \begin{bmatrix} 2-l + lr^{-2} & 0 & (2-l)\left(\frac{l}{l+1}\right)^{1/2}(1-r^{-2}) \\ 0 & 2r^{-1} & 0 \\ [l(1+l)]^{1/2}(1+r^{-2}) & 0 & l+(2-l)r^{-2} \end{bmatrix}. \tag{A.32}$$

The nonzero pressure fields associated with the solutions \mathbf{u}_{lmq}^\pm are

$$q_{lm0}^+ = \left(\frac{l+1}{l}\right)^{1/2} (2l+3)r^l Y_{lm}(\hat{\mathbf{r}}), \tag{A.33}$$

$$q_{lm2}^+ = -\frac{(l+1)(2l+3)}{l} r^l Y_{lm}(\hat{\mathbf{r}}), \tag{A.34}$$

$$q_{lm0}^- = \left(\frac{l}{l+1}\right)^{1/2} (2l-1)r^{-(l+1)} Y_{lm}(\hat{\mathbf{r}}), \tag{A.35}$$

$$q_{lm2}^- = \frac{l(2l-1)}{l+1} r^{-(l+1)} Y_{lm}(\hat{\mathbf{r}}). \tag{A.36}$$

Appendix B. Spherical tensor basis

Here, we list the complete set of orthonormal traceless tensors \mathbf{a}_{2m} , defined by Eq. (58):

$$\begin{aligned} \mathbf{a}_{20} &= \frac{1}{\sqrt{6}} \begin{pmatrix} -1 & 0 & 0 \\ 0 & -1 & 0 \\ 0 & 0 & 2 \end{pmatrix}, \\ \mathbf{a}_{21} &= \begin{pmatrix} 0 & 0 & -1/2 \\ 0 & 0 & -i/2 \\ -1/2 & -i/2 & 0 \end{pmatrix}, \quad \mathbf{a}_{2-1} = \begin{pmatrix} 0 & 0 & 1/2 \\ 0 & 0 & -i/2 \\ 1/2 & -i/2 & 0 \end{pmatrix}, \\ \mathbf{a}_{22} &= \begin{pmatrix} 1/2 & i/2 & 0 \\ i/2 & -1/2 & 0 \\ 0 & 0 & 0 \end{pmatrix}, \quad \mathbf{a}_{2-2} = \begin{pmatrix} 1/2 & -i/2 & 0 \\ -i/2 & -1/2 & 0 \\ 0 & 0 & 0 \end{pmatrix}. \end{aligned} \tag{B.1}$$

Appendix C. Matrices $X_{qq'}$ and W_q

The explicit expression for the matrix $X_{qq'}$ is [14,18]

$$X_{qq'} = -(2l+1) \times \begin{pmatrix} \frac{l(2l-1)(2l+1)(\lambda+2)}{(l+1)(1+\lambda)} & 0 & \frac{(2l-1)(2l+1)(2l+3)\lambda}{2(1+\lambda)} \\ 0 & \frac{l(l+1)(l-1)(\lambda-1)}{(l-1)\lambda+(l+2)} & 0 \\ \frac{(2l-1)(2l+1)(2l+3)\lambda}{2(1+\lambda)} & 0 & \frac{(l+1)(2l+1)^2(2l+3)((2l+1)\lambda-2)}{4l(1+\lambda)} \end{pmatrix}. \quad (C.1)$$

To derive the matrix representations of the operator $\widehat{\mathbf{W}}$, we consider the flow field \mathbf{u}^F generated by Marangoni stresses,

$$\mathbf{u}^F = \widehat{\mathbf{W}}\Gamma. \quad (C.2)$$

By spherical symmetry, the problem is diagonal in quantum numbers l and m . In addition,

$$\langle \mathbf{S}_{lmq} \delta_1 | \mathbf{u}^F \rangle = \alpha_{lm} \delta_{q0}, \quad (C.3)$$

where the $q = 1$ component is excluded by parity considerations [9], and the $q = 2$ component is excluded by boundary condition (21). Eq. (A.23) and the above relation imply that

$$\mathbf{u}^F(\mathbf{r}) = \alpha_{lm} [\theta(1-r) \mathbf{u}_{lm0}^+(\mathbf{r}) + \theta(r-1) \mathbf{u}_{lm0}^-(\mathbf{r})], \quad (C.4)$$

where $\theta(x)$ is the Heaviside step function.

Viscous tractions are linearly related to the velocity field,

$$\mathbf{t} = \widehat{\mathbf{T}}\mathbf{u}, \quad (C.5)$$

where the operator $\widehat{\mathbf{T}}$ is diagonal in quantum numbers l and m . For the velocity field

$$\mathbf{u}_{lm0}^\pm(\mathbf{r}) = U_{00}^\pm(l; r) \mathbf{S}_{lm0} + U_{02}^\pm(l; r) \mathbf{S}_{lm2}, \quad (C.6)$$

the corresponding tractions are

$$\mathbf{t} = r \frac{d}{dr} \left(\frac{U_{00}^\pm(l; r)}{r} \right) \mathbf{S}_{lm0} + \left(2 \frac{d}{dr} U_{00}^\pm(l; r) - q_{lm0}^\pm \right) \mathbf{S}_{lm2}, \quad (C.7)$$

where q_{lm0}^\pm is the pressure field (A.33) or (A.35). From (C.7) and (A.31)–(A.36), we find

$$\langle \mathbf{S}_{lm0} \delta_1 | \widehat{\mathbf{T}} | \mathbf{u}_{lm0}^+ \rangle = 2l + 1, \quad (C.8)$$

$$\langle \mathbf{S}_{lm0} \delta_1 | \widehat{\mathbf{T}} | \mathbf{u}_{lm0}^- \rangle = -(2l + 1), \quad (C.9)$$

$$\langle \mathbf{S}_{lm2} \delta_1 | \widehat{\mathbf{T}} | \mathbf{u}_{lm0}^+ \rangle = -3 \left(\frac{l+1}{l} \right)^{1/2}, \quad (C.10)$$

$$\langle \mathbf{S}_{lm2} \delta_1 | \widehat{\mathbf{T}} | \mathbf{u}_{lm0}^- \rangle = 3 \left(\frac{l}{l+1} \right)^{1/2}. \quad (C.11)$$

Eq. (C.4), tangential stress balance (23), and equation of state (24) yield

$$[\langle \mathbf{S}_{lm0} \delta_1 | \widehat{\mathbf{T}} | \mathbf{u}_{lm0}^- \rangle - \lambda \langle \mathbf{S}_{lm0} \delta_1 | \widehat{\mathbf{T}} | \mathbf{u}_{lm0}^+ \rangle] \alpha_{lm} = Ma \langle \mathbf{S}_{lm0} \delta_1 | \nabla | \bar{r} \rangle, \quad (\text{C.12})$$

which gives a relation between α_{lm} and γ_{lm}

$$\alpha_{lm} = -Ma \frac{[l(l+1)]^{1/2}}{(2l+1)\lambda_1} \gamma_{lm}. \quad (\text{C.13})$$

Eq. (76) is obtained from the above relation using (72), (C.2), and (C.3).

The induced force distribution associated with Marangoni stresses is the traction jump across the spherical surface at $r = 1$ in a uniform fluid ($\lambda = 1$) with velocity field \mathbf{u}^F . By Eq. (48), the corresponding reduced multipole moments are

$$f_{lmq}^F = - \sum_{q'=0,2} \langle \mathbf{v}_{lmq}^+ \delta_1 | \mathbf{S}_{lmq'} \rangle [\langle \mathbf{S}_{lmq'} \delta_1 | \widehat{\mathbf{T}} | \mathbf{u}_{lm0}^- \rangle - \langle \mathbf{S}_{lmq'} \delta_1 | \widehat{\mathbf{T}} | \mathbf{u}_{lm0}^+ \rangle] \alpha_{lm}, \quad (\text{C.14})$$

where the transformation matrix $\langle \mathbf{v}_{lmq}^+ \delta_1 | \mathbf{S}_{lmq'} \rangle$ is given by (70) and (A.26). From definition (51),(53), and Eqs. (C.8)–(C.11), (C.13), (C.14) we find

$$W_q(l) = -\frac{1}{\lambda_1} [l(2l-1), 0, \frac{1}{2}(l+1)(2l+1)(2l+3)]. \quad (\text{C.15})$$

Eq. (C.15) can alternatively be obtained from (76) by using (74) and (A.27).

Appendix D. Coupling between scalar and vector spherical harmonics

In Dirac notation, the vector-harmonic expansion of a product of vector and scalar harmonics has the form

$$|\mathbf{S}_{lmq} Y_{l'm'}\rangle = |\mathbf{S}_{l''m''q''}\rangle \langle \mathbf{S}_{l''m''q''} \delta_1 | \mathbf{S}_{lmq} Y_{l'm'}\rangle, \quad (\text{D.1})$$

where the $\langle \mathbf{S}_{l''m''q''} \delta_1 | \mathbf{S}_{lmq} Y_{l'm'}\rangle$ are Clebsch–Gordon coupling coefficients. Since the tangential ($q = 0, 1$) and normal $q = 2$ harmonics do not couple,

$$\langle \mathbf{S}_{l''m''2} \delta_1 | \mathbf{S}_{lmq} Y_{l'm'}\rangle = \langle \mathbf{S}_{l''m''q} \delta_1 | \mathbf{S}_{lm2} Y_{l'm'}\rangle = 0, \quad q = 0, 1. \quad (\text{D.2})$$

The nonzero coupling coefficients are [24]

$$\begin{aligned} \langle \mathbf{S}_{l''m''0} \delta_1 | Y_{l'm'} \mathbf{S}_{lm0} \rangle &= \langle \mathbf{S}_{l''m''1} \delta_1 | Y_{l'm'} \mathbf{S}_{lm1} \rangle \\ &= \beta \begin{pmatrix} l & l' & l'' \\ 0 & 0 & 0 \end{pmatrix} \frac{l(l+1) + l''(l''+1) - l'(l'+1)}{[l(l+1)l''(l''+1)]^{1/2}}, \end{aligned} \quad (\text{D.3})$$

$$\begin{aligned} \langle \mathbf{S}_{l''m''0} \delta_1 | Y_{l'm'} \mathbf{S}_{lm1} \rangle &= (-1)^{m'} \langle \mathbf{S}_{lm1} \delta_1 | Y_{l' -m'} \mathbf{S}_{l''m''0} \rangle \\ &= \beta \begin{pmatrix} l & l' & l'' - 1 \\ 0 & 0 & 0 \end{pmatrix} \left[\frac{(s+1)(s-2l)(s-2l')(s-2l''+1)}{l(l+1)l''(l''+1)} \right]^{1/2}, \end{aligned} \quad (\text{D.4})$$

and

$$\langle \mathbf{S}_{l''m''2} \delta_1 | Y_{l'm'} \mathbf{S}_{lm2} \rangle = \beta \begin{pmatrix} l & l' & l'' \\ 0 & 0 & 0 \end{pmatrix}, \quad (\text{D.5})$$

where

$$s = l + l' + l'', \quad (\text{D.6})$$

$$\beta = \frac{(-1)^{m''}}{2} \left(\frac{(2l+1)(2l'+1)(2l''+1)}{4\pi} \right)^{1/2} \begin{pmatrix} l & l' & l'' \\ m & m' & -m'' \end{pmatrix}, \quad (\text{D.7})$$

and

$$\begin{pmatrix} l & l' & l'' \\ m & m' & m'' \end{pmatrix}$$

is the Wigner $3j$ -symbol [23].

The $3j$ -symbol vanishes,

$$\begin{pmatrix} l & l' & l'' \\ m & m' & m'' \end{pmatrix} = 0, \quad (\text{D.8})$$

unless

$$m + m' + m'' = 0, \quad (\text{D.9})$$

and the triangular condition

$$\begin{aligned} -l + l' + l'' &\geq 0, \\ l - l' + l'' &\geq 0, \\ l + l' - l'' &\geq 0 \end{aligned} \quad (\text{D.10})$$

is satisfied. Also,

$$\begin{pmatrix} l & l' & l'' \\ 0 & 0 & 0 \end{pmatrix} = 0, \quad (\text{D.11})$$

unless

$$l + l' + l'' = 2k, \quad k = 1, 2, \dots \quad (\text{D.12})$$

Eq. (D.4) and conditions (D.10)–(D.12) imply diagonal coupling to rigid rotation around the z -axis

$$\langle \mathbf{S}_{lm0} \delta_1 | Y_{l'm'} \mathbf{S}_{l01} \rangle = \delta_{ll'} \delta_{mm'} \left(\frac{3}{8\pi} \right)^{1/2} \frac{m}{[l(l+1)]^{1/2}}. \quad (\text{D.13})$$

Appendix E. High-viscosity expansion

Eqs. (119), (120) imply that the general form of the coefficients in expansions (125)–(127) is

$$C_m = \frac{\sum_{i=1}^{n_1} a_i \tilde{M} a^{-b_i}}{\prod_{j=1}^{n_2} (1 + c_j^2 \tilde{M} a^{-2})^{d_j}} \quad (\text{E.1})$$

where $C_m = \tau'_{12}{}^{(m)}$, $N_1{}^{(m)}$ or $N_2{}^{(m)}$. The coefficients c_j and d_j are the same for all components of the stress tensor; the positions of the poles c_j do not depend on m , but the orders d_j are m dependent. Only finite numbers of terms n_1 and n_2 contribute to the numerator and denominator of (E.1) for each m . For $m < 5$, the nonzero expansion coefficients C_m are given by Eqs. (128)–(132); the parameters a_i , b_i , c_j , d_j for $m=5, 6$, and 7 are listed in Tables 1–4.

Table 1
Coefficients c_j and d_j in the denominator of Eq. (E.1)

j	c_j	d_j		
		$m = 5$	$m = 6$	$m = 7$
1	5/6	5	4	7
2	9/10	2	2	3
3	9/20	1	2	2
4	13/14	1	1	2
5	13/42	1	1	2
6	13/21	0	1	1
7	17/18	0	0	1
8	17/36	0	0	1

Table 2
Coefficients a_i and b_i in the numerator of Eq. (E.1) for $m = 5$

$\tau'_{12}{}^{(5)}$ b_i	a_i	$N_1{}^{(5)}$	
		b_i	a_i
6	-1.1131	5	0.3570
8	3.6160	7	-5.7812
10	1.9948	9	2.7328
12	-1.5908	11	6.0089
14	-0.3417	13	-0.2007
16	2.6853×10^{-2}	15	-0.3754
18	4.1725×10^{-3}	17	-2.0219×10^{-2}
		19	8.4949×10^{-4}

Table 3
Coefficients a_i and b_i in the numerator of Eq. (E.1) for $m = 6$

$N_2{}^{(6)}$ b_i	a_i
7	0.37806
9	-0.12507
11	-0.75966
13	-0.42562
15	-6.4450×10^{-2}
17	3.4703×10^{-3}
19	1.0453×10^{-3}
21	4.2491×10^{-5}

Table 4
Coefficients a_i and b_i in the numerator of Eq. (E.1) for $m = 7$

$\tau'_{12}{}^{(7)}$		$N_1'{}^{(7)}$	
b_i	a_i	b_i	a_i
8	-1.3772	7	0.2777
10	11.671	9	-11.426
12	14.468	11	16.618
14	-29.788	13	80.369
16	-55.012	15	42.472
18	-21.216	17	-55.718
20	9.6628	19	-65.766
22	9.4622	21	-19.127
24	2.2531	23	3.2719
26	-4.9502×10^{-2}	25	2.9926
28	-0.10447	27	0.5959
30	-1.6134×10^{-3}	29	2.6721×10^{-2}
32	-7.0468×10^{-4}	31	-5.2951×10^{-3}
34	2.7259×10^{-5}	33	-6.5709×10^{-4}

According to Eq. (127)

$$N_2^{(m)} = -\frac{1}{2}N_1^{(m)} \quad (\text{E.2})$$

for odd m .

Appendix F. Low-Marangoni-number behavior

F.1. Trajectory analysis

For $Ma = 0$, surfactant is passively convected on the drop interface. Evolution of surfactant along a streamline on the interface is described by the trajectory equations

$$\frac{d\varphi}{dt} = \frac{u_\varphi}{\sin\theta}, \quad (\text{F.1})$$

$$\frac{d\theta}{dt} = u_\theta, \quad (\text{F.2})$$

and the continuity equation

$$\frac{D\Gamma}{Dt} = -\Gamma\nabla_s \cdot \mathbf{u}_s, \quad (\text{F.3})$$

where u_φ and u_θ are the spherical components of the interfacial velocity \mathbf{u}_s , and D/Dt is the material derivative.

For two-dimensional external flows (135),

$$u_\varphi = \frac{1}{2}[\lambda_1^{-1}\cos(2\varphi) - \alpha]\sin\theta, \quad (\text{F.4})$$

$$u_\theta = \frac{1}{4}\lambda_1^{-1}\sin(2\theta)\sin(2\varphi), \quad (\text{F.5})$$

and

$$\nabla_s \cdot \mathbf{u}_s = -\frac{3}{2}\lambda_1^{-1} \sin(2\varphi) \sin^2\theta. \tag{F.6}$$

With these expressions, integration of (F.1) and (F.2) yields the trajectory equation (137), and a subsequent integration of (F.3) yields the stationary surfactant concentration (136).

F.2. Expansion in Ma

Here, we illustrate certain features of the hierarchy (144) and (145) by constructing an approximate solution in the subspace of spherical harmonics with $l = 2$. In this subspace, with shear flow (62), hierarchy (144) and (145) reduces to

$$A_{2m2m'}\gamma_{2m'}^{(i)} + \sigma_{2m}^{(i)} = 0, \quad i = 1, 2, \dots \tag{F.7}$$

where

$$A_{2m2m'} = i \begin{bmatrix} -1 & -b\lambda_1^{-1} & 0 \\ b\lambda_1^{-1} & 0 & -b\lambda_1^{-1} \\ 0 & b\lambda_1^{-1} & 1 \end{bmatrix}, \quad b = \frac{1}{7}\left(\frac{3}{2}\right)^{1/2}, \tag{F.8}$$

$$\sigma_{2m}^{(0)} = i \left(\frac{6\pi}{5}\right)^{1/2} \lambda_1^{-1} \begin{bmatrix} 1 \\ 0 \\ -1 \end{bmatrix}, \tag{F.9}$$

and

$$\sigma_{2m}^{(j)} = -\frac{6}{5}\lambda_1^{-1} \begin{bmatrix} \gamma_{2-2}^{(j-1)} \\ \gamma_{20}^{(j-1)} \\ \gamma_{22}^{(j-1)} \end{bmatrix} + \frac{6}{7}(5\pi)^{-1/2} \lambda_1^{-1} \sum_{k=0}^{j-1} \begin{bmatrix} \gamma_{2-2}^{(k)} \gamma_{20}^{(j-1-k)} \\ \gamma_{2-2}^{(k)} \gamma_{22}^{(j-1-k)} - 2\gamma_{20}^{(k)} \gamma_{20}^{(j-1-k)} \\ \gamma_{20}^{(k)} \gamma_{22}^{(j-1-k)} \end{bmatrix} \tag{F.10}$$

for $j \geq 1$. In Eqs. (F.8)–(F.10) the order of indices is $m, m' = -2, 0, 2$.

From Eq. (F.8),

$$\det |A_{2m2m'}| = 0. \tag{F.11}$$

For $i = 0$, Eq. (F.7) has a family of solutions

$$\gamma_{22}^{(0)} = \gamma_{2-2}^{(0)} = \lambda_1^{-1} \left[\left(\frac{6\pi}{5}\right)^{1/2} - \frac{1}{7} \left(\frac{3}{2}\right)^{1/2} \gamma_{20}^{(0)} \right], \tag{F.12}$$

where $\gamma_{20}^{(0)}$ is arbitrary. At the next perturbation level, the solubility condition of Eq. (F.7) with $i = 1$ is

$$\gamma_{20}^{(0)}(c_1\gamma_{20}^{(0)} + c_2) = 0, \tag{F.13}$$

where

$$c_1 = -\frac{3}{343\sqrt{5\pi}}(3 + 49\lambda_1^2), \quad c_2 = \frac{6}{245}(3 - 49\lambda_1^2). \tag{F.14}$$

The solution $\gamma_{20}^{(0)} = -c_2/c_1$ is unphysical, because it yields negative surfactant concentration; thus,

$$\gamma_{20}^{(0)} = 0 \quad (\text{F.15})$$

according to Eq. (F.13). This procedure can be continued recurrently to generate the solution

$$\gamma_{2\pm 2}^{(i)} = (\mp i)^i \left(\frac{6}{5}\right)^{i+1/2} \pi^{1/2} \lambda_1^{-(i+1)}, \quad (\text{F.16})$$

$$\gamma_{20}^{(i)} = 0. \quad (\text{F.17})$$

The corresponding expansions of the shear and normal stresses are

$$\tau_{12}^r = \frac{3}{2} \sum_{k=1}^{\infty} (-1)^{k+1} \left(\frac{6Ma}{5\lambda_1}\right)^{2k}, \quad (\text{F.18})$$

$$N_1 = 3\lambda_1^{-1} \sum_{k=1}^{\infty} (-1)^{k+1} \left(\frac{6Ma}{5\lambda_1}\right)^{2k-1}, \quad (\text{F.19})$$

$$N_2 = -\frac{1}{2}N_1. \quad (\text{F.20})$$

Expressions (F.18)–(F.20) are equivalent to the $O(\lambda_1^{-1})$ terms (128) and (130) in expansions (125)–(127) (Figs. 1–5).

The foregoing analysis was extended to matrices truncated at $l=2k$, where $k=2, 3$. In each case, a similar structure was found that involves k coupled quadratic consistency conditions, and a leading-order solution depending on k constants.

References

- [1] P.R. Borwankar, S.E. Case, Rheology of emulsions, foams and gels, *Curr. Opin. Colloid Interface Sci.* 2 (1997) 584–589.
- [2] F. Lequeux, Emulsion rheology, *Curr. Opin. Colloid Interface Sci.* 3 (1998) 408–411.
- [3] M.D. Lacasse, G.S. Grest, D. Levine, T.G. Mason, D.A. Weitz, Model for the elasticity of compressed emulsions, *Phys. Rev. Lett.* 76 (1996) 3448–3451.
- [4] T.G. Mason, M.D. Lacasse, G.S. Grest, D. Levine, J. Bibette, D.A. Weitz, Osmotic pressure and viscoelastic shear moduli of concentrated emulsions, *Phys. Rev. E* 56 (1997) 3150–3166.
- [5] P. Hebraud, F. Lequeux, Mode-coupling theory for the pasty rheology of soft glassy materials, *Phys. Rev. Lett.* 81 (1998) 2934–2937.
- [6] M. Loewenberg, E.J. Hinch, Numerical simulations of a concentrated emulsion in shear flow, *J. Fluid. Mech.* 321 (1996) 395–419.
- [7] R. Charles, C. Pozrikidis, Significance of the dispersed-phase viscosity on the simple shear flow of suspensions of two-dimensional liquid drops, *J. Fluid Mech.* 365 (1998) 205–234.
- [8] J.F. Paliarne, Linear rheology of viscoelastic emulsions with interfacial tension, *Rheol. Acta* 29 (1990) 204–214. *Correction Rheol. Acta* 30 (1991) 497–497.
- [9] J. Bławdziewicz, E. Wajnryb, M. Loewenberg, Hydrodynamic interactions and collision efficiencies of spherical drops covered with an incompressible surfactant film, *J. Fluid Mech.* (1999) in press.
- [10] X. Li, C. Pozrikidis, The effect of surfactants on drop deformation and on the rheology of dilute emulsions in Stokes flow, *J. Fluid Mech.* 341 (1997) 165–194.
- [11] S. Yon, C. Pozrikidis, A finite-volume/boundary-element method for flow past interfaces in the presence of surfactants, with application to shear flow past a viscous drop, *Comput. Fluids* 27 (1998) 879–902.

- [12] J. Bławdziewicz, V. Cristini, M. Loewenberg, Stokes flow in the presence of a planar interface covered with incompressible surfactant, *Phys. Fluids* 11 (1999) 251–258.
- [13] V. Cristini, J. Bławdziewicz, M. Loewenberg, Near-contact motion of surfactant-covered spherical drops, *J. Fluid Mech.* 366 (1998) 259–287.
- [14] B. Cichocki, B.U. Felderhof, R. Schmitz, Hydrodynamic interactions between two spherical particles, *PhysicoChem. Hyd.* 10 (1988) 383–403.
- [15] R.G. Cox, H. Brenner, *J. Fluid Mech.* 28 (1967) 391.
- [16] P. Mazur, D. Bedeaux, *Physica A* 76 (1974) 235.
- [17] R. Schmitz, B.U. Felderhof, Creeping flow about a spherical particle, *Physica A* 113 (1982) 90–102.
- [18] R.B. Jones, R. Schmitz, Mobility matrix for arbitrary spherical particles in solution, *Physica A* 149 (1988) 373–394.
- [19] G.I. Taylor, The viscosity of a fluid containing small drops of another fluid, *Proc. Roy. Soc. A* 138 (1932) 41.
- [20] P. Vlahovska, J. Bławdziewicz, M. Loewenberg, Manuscript in preparation.
- [21] D. Barthès-Biesel, A. Acrivos, Deformation and burst of a liquid droplet freely suspended in a linear shear field, *J. Fluid Mech.* 61 (1973) 1–21.
- [22] J.M. Rallison, Note on the time-dependent deformation of a viscous drop which is almost spherical, *J. Fluid Mech.* 98 (1980) 625–633.
- [23] A.R. Edmonds, *Angular Momentum in Quantum Mechanics*, Princeton University Press, Princeton, 1960.
- [24] M.N. Jones, *Spherical Harmonics and Tensors for Classical Field Theory*, Wiley, New York, 1985.